VYSOKÉ UČENÍ TECHNICKÉ V BRNĚ

BRNO UNIVERSITY OF TECHNOLOGY

FAKULTA STROJNÍHO INŽENÝRSTVÍ

FACULTY OF MECHANICAL ENGINEERING

ÚSTAV MATERIÁLOVÝCH VĚD A INŽENÝRSTVÍ

INSTITUTE OF MATERIALS SCIENCE AND ENGINEERING

DEPOZICE BIOAKTIVNÍCH KERAMICKÝCH VRSTEV POMOCÍ TECHNOLOGIE RF-ICP

RF-ICP DEPOSITION OF BIOACTIVE HYDROXYLAPATITE COATINGS

DIPLOMOVÁ PRÁCE

DIPLOMA THESIS

AUTOR PRÁCE — **Bc. DANIEL DUKOVSKÝ**

AUTHOR

VEDOUCÍ PRÁCE — **Ing. JAN ČÍŽEK, Ph.D.**

SUPERVISOR

BRNO 2021

BRNO UNIVERSITY OF TECHNOLOGY
FACULTY OF MECHANICAL ENGINEERING

Assignment Master's Thesis

Institut:	Institute of Materials Science and Engineering
Student:	**Bc. Daniel Dukovský**
Degree programm:	Applied Sciences in Engineering
Branch:	Materials Engineering
Supervisor:	**Ing. Jan Čížek, Ph.D.**
Academic year:	2020/21

As provided for by the Act No. 111/98 Coll. on higher education institutions and the BUT Study and Examination Regulations, the director of the Institute hereby assigns the following topic of Master's Thesis:

RF–ICP deposition of bioactive hydroxylapatite coatings

Brief Description:

RF–ICP (radio frequency inductively–coupled plasma) is a novel technology, unique in the Czech Republic, capable of deposition of non–oxidized coatings onto substrates. Owing to its advantages, the technology was proposed for a future use in biomaterials applications.

There are several papers in the literature on deposition and characterization of hydroxyapatite–based ceramics. The task of the student will be deposition of hydroxyapatite (HA) onto Ti6Al4V alloy substrates using RF–ICP technology under different selected spray conditions (such as torch power, powder feedrate, gas pressure) and a subsequent analysis of the coatings in terms of their microstructure and chemical/phase composition.

Master's Thesis goals:

– literature review of basic principles and features of RF–ICP technology,
– deposit HA coatings using RF–ICP at different spray conditions (e.g. torch power, powder feedrate, chamber pressure),
– analyze microstructure and chemical/phase composition of the fabricated coatings.

Recommended bibliography:

DAVIS, J. R. Handbook of Thermal Spray Technology. ASM International, 338p, 2004. ISBN: 978--61503-996-8.

BOULOS, M. I. New frontiers in thermal plasmas from space to nanomaterials. Nuclear Engineering and Technology, vol. 44(5), pp.1-8, 2012. DOI : 10.5516/NET.77.2012.001.

Tekna Systems. SY170 15kW induction plasma system original operating manual, 98p, 2017.

INAGAKI, M., YOKOGAWA, Y., KAMEYAMA, T.: Effects of plasma gas composition on bond strength of hydroxyapatite/titanium composite coatings prepared by RF-plasma spraying. Journal of the European Ceramic Society, vol. 26(4-5), pp. 495-499, 2006.

ROY, M., BANDYOPADHYAY, A., BOSE, S.: Induction plasma sprayed nano hydroxyapatite coatings on titanium for orthopaedic and dental implants. Surface and Coatings Technology, vol. 205(8-9), pp. 2785-2792, 2011.

NELEA, V., MOROSANU, C., ILIESCU, M., MIHAILESCU, I.N.: Microstructure and mechanical properties of hydroxyapatite thin films grown by RF magnetron sputtering. Surface and Coatings Technology, vol. 173(2-3), pp. 315-322, 2003.

Deadline for submission Master's Thesis is given by the Schedule of the Academic year 2020/21

In Brno,

L. S.

prof. Ing. Ivo Dlouhý, CSc.	doc. Ing. Jaroslav Katolický, Ph.D.
Director of the Institute	FME dean

Abstrakt
Tato diplomová práce se zabývá problematikou plazmového nanášení bioaktivních keramických povlaků hydroxylapatitu s využitím technologie radio-frekvenčně buzeného indukčně vázaného plazmatu. Cílem bylo optimalizovat proces a nanést kompaktní hydroxylapatitové povlaky na substráty z titanové slitiny Ti6Al4V. Nanesené vzorky byly následně podrobeny analýzám povrchové drsnosti, mikrostruktury a fázového složení. Ze získaných výsledků byly vyvozeny závěry, které byly srovnány s dalšími odbornými pracemi zabývajícími se příbuznou problematikou.

Abstract
This diploma thesis deals with the topic of plasma spray deposition of bioactive ceramic coatings, specifically hydroxylapatite, using radio frequency inductively-coupled plasma technology. The aim was to optimize the deposition process and develop compact hydroxylapatite coatings on titanium alloy Ti6Al4V substrates. The deposited samples were then subjected to analyzes in terms of surface roughness, microstructure and phase composition. Conclusions were derived from the obtained results, which were compared with other scientific works dealing with related topic.

Klíčová slova
Radio-frekvenčně buzené indukčně vázané plazma, RF-ICP, hydroxylapatit, HA, titanová slitina, Ti6Al4V.

Keywords
Radio frequency inductively-coupled plasma, RF-ICP, hydroxylapatite, HA, titanium alloy, Ti6Al4V.

DUKOVSKÝ, D. *Depozice bioaktivních keramických vrstev pomocí technologie RF-ICP.* Brno: Vysoké učení technické v Brně, Fakulta strojního inženýrství, 2021. 64 s. Vedoucí diplomové práce Ing. Jan Čížek, Ph.D.

Rozšířený abstrakt

Stejně jako okolní svět, i lidské tělo podléhá působení času a pozvolné degradaci jednotlivých částí organismu. Pomineme-li zranění způsobená nehodami či vážnými nemocemi, tak především s rostoucí průměrnou délkou života roste i počet lidí, u nichž je nezbytně nutný zásah do organismu za účelem opravit nebo vyměnit část, která již není schopná plnit svoji funkci a omezuje člověka v plnohodnotném životě.

Z tohoto důvodu vyvstala potřeba zkoumat a objevovat materiály vhodné k náhradě nebo podpoře jednotlivých částí lidského těla. Takové materiály označujeme jako biomateriály, jelikož jsou použity v biologickém systému, který nesmějí nijak narušovat. Nesmějí způsobovat imunitní reakce, nesmějí být toxické či karcinogenní. Z tohoto pohledu dnes existuje celá řada biomateriálů zasahující do všech materiálových kategorií od polymerů, přes kovy a keramiky, až po složené kompozity.

Ačkoliv se mnoho problémů spojených s aplikacemi biomateriálů podařilo v průběhu času vyřešit, stále existují oblasti, které poskytují prostor pro zlepšení a vyžadují další výzkum. V návaznosti na to byla vypracována i tato diplomová práce, která se zabývá depozicí bioaktivní keramiky, konkrétně hydroxylapatitu, na bioinertní titanovou slitinu Ti6Al4V. Tato kombinace se nejčastěji používá pro výrobu endoprotéz, tedy ortopedických náhrad nejčastěji kyčelních a kolenních kloubů.

Pro vytvoření vrstev bioaktivních keramických materiálů na kovových implantátech se používají technologie žárového nanášení, konkrétně plazmové nanášení, jakožto jediná povolená depoziční metoda schválená příslušnými orgány. Nicméně v rámci této technologické třídy existuje několik procesů, které mohou dnes komerčně nanášeným hydroxylapatitovým povlakům poskytnout jiné, v ideálním případě lepší, bioaktivní či mechanické vlastnosti. Jedním z těchto procesů je i technologie radio-frekvenčně buzeného indukčně vázaného plazmatu (RF-ICP), která zde byla použita pro depozici povlaků a jejíž výsledky tato diplomová práce prezentuje a diskutuje.

V úvodu experimentu bylo nutné stanovit parametry depozice, jako např. výkon hořáku, podávací rychlost či depoziční vzdálenost. Tomuto účelu posloužily substráty z korozivzdorné oceli AISI 304. Optimalizace procesu začala s výkonem 9 kW a postupně byly vzorky deponovány při výkonech 12 a 15 kW, což je zároveň nejvyšší možný výkon použitého zařízení RF-ICP (Tekna Tek-15). Pro depozici prvních tří vzorků byl zvolen lineární posun substrátů ve směru kolmém k ose plazmového nanášení a podávané množství prášku bylo nastaveno na 0,15 g/min. Depozice těchto vzorků se lišila pouze použitým výkonem, nicméně z hlediska mikrostruktury došlo k výrazným změnám. Povlak prvního vzorku obsahoval velké množství neprotavených částic, následkem čehož byla vysoká porozita a potenciálně tedy špatné mechanické vlastnosti. Povlak druhého vzorku byl kompaktnější, méně porézní, ale stále jevil nevyhovující obsah neprotavených částic. Třetí vzorek získal povlak složený z dobře protavených částic, zato byl téměř neporézní. Takováto struktura však není zcela vhodná pro ortopedické aplikace, proto byl proces dále optimalizován. Maximální výkon byl ponechán, podávané množství prášku bylo zvýšeno na 1,3 g/min a k posuvnému pohybu substrátu se připojil pohyb rotační. Při těchto podmínkách byl deponován čtvrtý vzorek, který z mikrostrukturního hlediska vyhovoval počátečním požadavkům. Tím byl dokončen proces optimalizace depozičních parametrů.

Na základě získaných dat se přistoupilo k depozici na titanové slitiny Ti6Al4V. Pátý vzorek byl tedy s výjimkou materiálu substrátu deponován při stejných podmínkách jako čtvrtý. Mikrostruktura povlaků obou vzorků se, dle očekávání, velmi podobala. Pro

srovnání byl vytvořen poslední, šestý vzorek. Depoziční vzdálenost byla zvýšena ze 70 mm na 110 mm a podávané množství prášku bylo sníženo na 0,65 g/min. Úprava těchto parametrů měla ovlivnit množství neprotavených částic v povlaku, čehož bylo úspěšně dosaženo. Nicméně všechny připravené povlaky obsahovaly vertikální trhliny, které se nepodařilo úpravou zmíněných parametrů odstranit. Přítomnost vertikálních trhlin není z pohledu možného přístupu tělních tekutin k materiálu substrátu ani mechanických vlastností žádoucí. V tomto ohledu je naplánováno další pokračování tohoto výzkumu, které tento nedostatek pomůže odstranit.

Povrchová drsnost byla u všech vzorků v rozmezí 16-17,3 μm. Ideální povrchová drsnost pro adhezi, diferenciaci buněk a jejich růst se pohybuje okolo 5 μm, nicméně drsnost dostatečná pro adhezi a růst osteoblastů je v rozmezí 20-50 μm. Z tohoto pohledu bylo možné povrchovou drsnost všech vzorků označit jako vyhovující.

Obrazovou analýzou s využitím softwaru ImageJ byla stanovena porozita a velikost pórů. Porozita vzorků se pohybovala v rozmezí 8,5-10,8 %, přičemž ideální porozita plazmově nanášených povlaků by se měla pohybovat v rozmezí 5-20 %, aby zůstaly zachovány dostatečné mechanické vlastnosti. Pro vrůstání kostní tkáně je žádoucí vysoká porozita a velikost pórů alespoň 50 μm. V případě zkoumaných vzorků se velikost pórů pohybovala od 24 do 34 μm. Z tohoto pohledu byla velikost pórů u všech vzorků spíše nedostatečná a nevhodná pro vrůstání kostní tkáně. Dosažení optimálních hodnot velikosti pórů je však obtížné pro více druhů plazmového nanášení.

Fázovou analýzou s využitím metody rentgenové difrakce (XRD) bylo stanoveno množství přítomného HA a dalších fází vzniklých vysokoteplotní dekompozicí HA v průběhu depozice. Výsledné povlaky obsahovaly 35-45 % HA fáze, zbývající obsah tvořily přeměněné fáze α-TCP, TTCP a CaO. Všechny tyto fáze jsou v lidském organismu rozpustnější než HA a tím mohou urychlovat degradaci povlaku. Navíc TTCP a CaO mohou být ve zvýšeném množství škodlivé.

Hydroxylapatitové povlaky titanových slitin se komerčně vyrábí za použití atmosférického plazmového nanášení. I s využitím této technologie dochází k dekompozici HA, nicméně výsledné povlaky si zachovávají výrazně vyšší obsah HA a akceptovatelné množství přeměněných fází. Ve světle těchto skutečností se prozatím použití RF-ICP depozice nejeví jako výhodné. Optimalizace procesu proto bude nadále předmětem dalšího výzkumu za účelem dosažení povlaků blížících se svými vlastnostmi povlakům deponovaným komerčně využívanými technologiemi.

Prohlašuji, že jsem diplomovou práci na téma *Depozice bioaktivních keramických vrstev pomocí technologie RF-ICP* vypracoval samostatně pod vedením Ing. Jana Čížka, Ph.D. a použil jsem pouze uvedené prameny a literaturu.

. . . . . .
Bc. Daniel Dukovský
20. května 2021

Na tomto místě bych rád poděkoval svému vedoucímu práce Ing. Janu Čížkovi, Ph.D. za jeho odborný a přátelský přístup, cenné rady a připomínky, které mi pomohly k vypracování diplomové práce. Taktéž mé poděkování patří kolegům Ing. Jakubu Klečkovi a RNDr. Františku Lukáčovi, Ph.D. z Ústavu fyziky plazmatu AV ČR a Mgr. Janu Čuperovi z VUT FSI za spolupráci a pomoc při experimentálních měřeních. V neposlední řadě bych rád poděkoval své partnerce, přátelům a především rodičům za podporu v průběhu celého studia na vysoké škole.

Bc. Daniel Dukovský

Contents

1 Introduction

As well as the surrounding world, the human body is also subjected to the effects of time and a gradual degradation of individual parts of the body. Beside the injuries caused by accidents or serious illnesses, due to increasing life expectancy, the number of people needing intervention in their body to repair or replace a part that is no longer able to perform its function and restricts a person's full life, is increasing.

For this reason, there is a need to continue with research and discovering materials suitable for replacing or supporting the affected parts of the body. These materials are referred to as biomaterials as they are used in a biological system with which they cannot interfere. They cannot be toxic or carcinogenic or cause immune reactions. From today's perspective, there are a number of biomaterials reaching all material categories, ranging from polymers, to metals, and ceramics, or their composites.

Although many of the problems associated with biomaterial applications have been resolved over time, there are still areas that provide room for improvement and require further research. Following this, the present diploma thesis was prepared to attempt the deposition of bioactive ceramics, specifically hydroxylapatite, on the bioinert titanium alloy Ti6Al4V using a novel technology. This combination of materials is most often used for orthopedic applications, primarily for hip and knee replacements.

Plasma spray is an established technology for the production of endoprostheses. Within this technological class, there are currently several processes that can provide commercially applied hydroxylapatite coatings. One of these processes is the radio frequency inductively-coupled plasma technology, which was used for the deposition of coatings and its results are presented and discussed in this thesis.

2 Literature review

This part of the diploma thesis deals with the theoretical description of thermal spray methods, in particular the technology of radio frequency inductively-coupled plasma (RF-ICP). Considering the assignment of the diploma thesis, biocompatible coatings are then discussed. The group of biomaterials includes many different materials, and this work will deal mainly with bioceramic materials, with special attention to hydroxylapatite.

2.1 History and presence of surface engineering

Surface engineering as an independent discipline was officially commenced in 1983 at Birmingham University of Technology with the establishing of the first Surface Engineering Research Institute. Two years later, in 1985, the international Journal of Surface Engineering was first issued [1].

Surface engineering covers a very wide range of processes and technologies dealing with surface modifications and surface coatings, as shown in Fig. 2.1. It provides a valuable tool for inducing exceptional properties that cannot be achieved by using the material alone. Owing to this, surface engineering has rightfully gained the attention of industry. Surface modifications and surface coatings have thus found applications in many industrial fields such as fabrication of parts, mechanics, transport, catalysis, energy, production, microelectronics, etc. Among other things, one of the tasks of surface engineering is also to provide protection against corrosion, oxidation or wear, ensure possible biocompatibility, adhesion, durability, or toughness. [2].

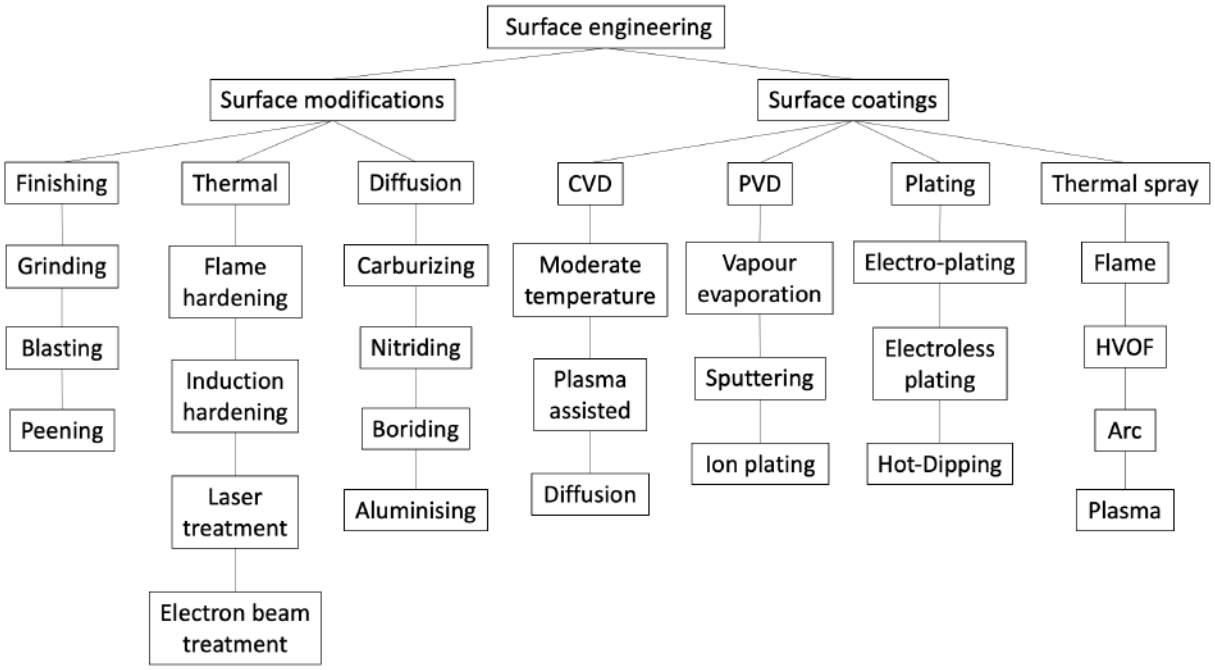

Figure 2.1: Schematic division of surface engineering methods [3]

Apparently, surface engineering spans a large number of processes, from those that modify the surface without any composition change, through processes causing a change in composition, to processes used for coating applications. Examples of the processes range from transformation hardening and surface texturing, through carburizing or nitriding, to electro-plating, thermal spraying and physical or chemical vapor depositions. The large range of methods also covers a very wide range of different materials [4].

2.1.1 Selected technologies of surface coatings

Surface engineering dealing with surface coatings has gone through three stages of interest since its inception. The first stage was the development of technologies for applying simple coatings. These technologies included thermal spraying, electro-plating, physical vapor deposition (PVD) and chemical vapor deposition (CVD), and other surface modification treatments such as laser treatment, etc. The second stage focused its interest on combining already known technologies in order to create coatings whose properties exceed the theoretical combination of methods, assuming a synergistic effect of 1+1>2. For example, a combination of thermal spraying - laser remelting, or electro-plating - surface treatment. The third stage was nano-surface engineering, a field dealing with nano-coatings and nano-materials and technologies related to them [1].

The graph in Fig. 2.2 compares selected coating technologies depending on the range of achievable coating thicknesses and typical temperatures recorded on the surface of a substrate. Four common coatings deposition processes (Fig. 2.1) will be discussed here in more detail: CVD, PVD, electro-plating, and thermal spraying. Due to its importance and considering the topic of this thesis, the latter will be discussed in more detail in a dedicated section 2.2.

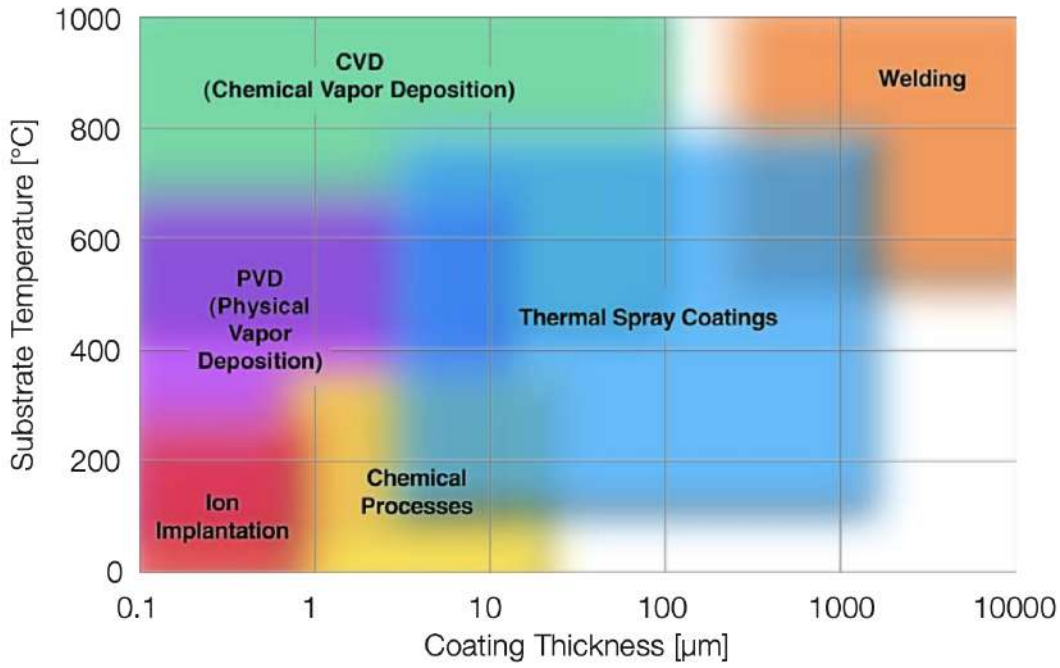

Figure 2.2: Technological limits of selected coating technologies (temperature loading of the substrate and maximum achievable thickness) [5]

- **Chemical vapor deposition (CVD)** forms coatings from chemically reactive gases, such as $TiCl_4$, $AlCl_3$, CH_4. The reaction temperatures can reach up to 1500 °C. However, the deposition process usually takes place at lower temperatures of 700-1100 °C and pressures of 1-100 kPa. The process requires gaseous reactants to contain a stable compound which would still be chemically decomposed due to the supply of energy (heating, plasma arc, laser), e.g., $TiCl_4$. The products of the decomposition are then deposited on the heated surface, where they act as a catalyst. In order for the required reaction to take place, the gases must also contain a non-metallic reactive gas (N_2, NH_4, CH_4). A heterogeneous reaction causes the formation of the layer on the substrate's surface. Two types of reactors are most often used - a hot-wall reactor and a cold-wall reactor. In the former, the reactor vessel and the substrate are heated simultaneously, thus maintaining the same temperature of the reactor's wall and the substrate. However, this solution has a disadvantage due to the coating also forming on the reactor's wall which could induce chemical reactions with the wall's material and contaminate the coating on the substrate. For this reason, this concept is only used for exothermic reactions, where the high temperature of the wall prevents the formation of a coating on its surface. Contrary to this, the second type of reactor is used for endothermic reactions. Only the holder with the substrate is heated, and, as the wall is usually cooled by water, no coating is formed elsewhere [6][7].

- As opposed to CVD, **physical vapor deposition (PVD)** is a method based on physical principles, vapor deposition or sputtering of solid materials on the surface of substrates at temperatures in the range of 150-500 °C in high vacuum environment ranging from 0.1-1 Pa. The coating is formed due to the condensation of atoms. PVD coatings are generally thinner than the same coatings deposited using CVD. Nowadays, three different PVD technologies are used the most often. The first type is sputtering, where the basic mechanism is the release of particles by the action of accelerated Ar ions. The second type is vapor evaporation, where the release of particles occurs due to the action of a low-voltage arc, laser, electron beam or induction. The released particles are ionized and react with the chamber's atmosphere formed by inert and reactive gas. The third method is ion plating, which utilizes concurrent or periodic bombardment of the substrate's surface and deposit atoms of material using atomic-sized energetic particles. The PVD method is the most ecological method of layer deposition, as no toxic substances are used or released during the deposition process. The advantage is the ability to coat even sharp edges. However, the disadvantage of all PVD methods is the need for a relatively complex vacuum system and the ability to coat only the surfaces lying in line-of-sight. Therefore, it is necessary to move the coated object during deposition in order to guarantee a compact coating [6][8][9].

- **Electro-plating** is also referred to as electrodeposition. During the process, a coating material is deposited onto the surface of the substrate using an electric current. Electro-plating is primarily used to change the physical properties such as corrosion or wear resistance. It is often used only for aesthetic reasons, when a thin layer of metal is applied to a cheap material to make it look more valuable. Generally, four primary components are needed to carry out the process - anode (positively charged electrode forming the plating), cathode (negatively charged electrode that is plated

- the substrate), solution (electrolytic solution where the reaction takes place; usually contains one or more metal salts), power source (electric current is added to the circuit to initiate the reaction). Once the electrodes are in the electrolyte and are connected, a direct current can flow between them towards the anode. This causes the anode to oxidize, which begins to dissolve into positive ions. These positive ions are then carried by the current to the negatively charged surface of the cathode, where they form a coating. Electro-plating occurs usually with metals or their alloys providing additional value to the substrate. Among the most frequently electrodeposited metals are Cu, Zn, Sn, Ni, Au, Ag or Pd [10].

2.2 Thermal spray technology

The first mention of thermal spray coating of components comes from the early 80s of the 19th century from Oerlikon (part of Zurich). The idea itself was subsequently evolved at the beginning of the next century by the Swiss engineer Max Ulrich Schoop. In 1909 he introduced the first commercially usable device for applying metal coatings. In the following years, he developed the technology of flame spraying, registered several patents and continued to research, among other things, coatings deposited by a plasma stream [11].

In the 1980s, the second boom in the development of thermal spraying came as other, more advanced technologies saw the light of day, such as vacuum plasma spraying (VPS), low pressure plasma spraying (LPPS) and high-velocity oxygen fuel spraying (HVOF) [12].

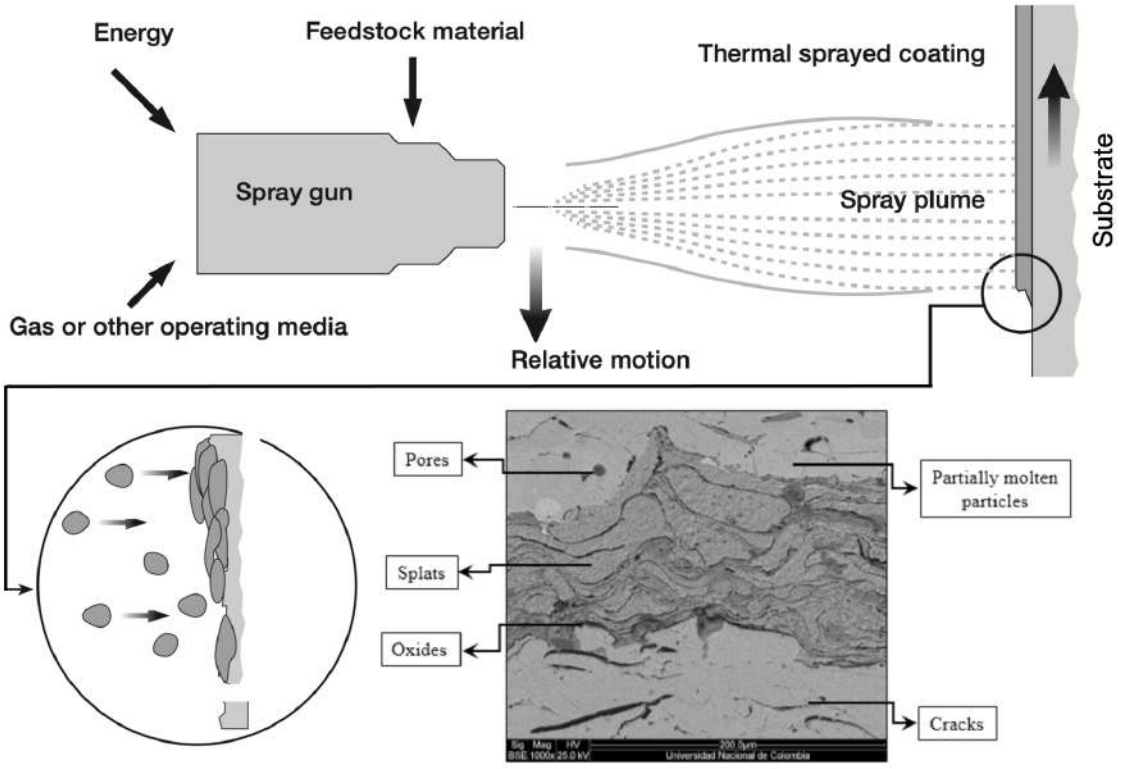

Figure 2.3: Scheme of a thermal spray coating process and typical coating microstructure [5][13]

The core and the essence of thermal spray deposition is melting of the coating material, a subsequent transport of the molten particles, and their adhesion to the surface of a substrate in order to form the coating upon their solidification (Fig. 2.3). Individual thermal spray technologies use different heat sources, either an electric energy or a flame. The coating material can be introduced in the form of rod, wire, powder, or suspension. In more detail, due to heat input, the semi-molten or molten particles (droplets, in fact) of coating material begin to form, and are subsequently transported to the substrate at high speeds. This causes the particles to deform upon impact and create pancake-shape formations on the substrate called splats. Heat from the hot particles is transferred to the cooler base material. As the particles solidify, they bond to the roughened base material. Adhesion of the coating is therefore mostly based on mechanical bonding [5][14].

Thermal spray processes reach one of the highest temperatures among other coating technologies. Therefore, it is necessary to choose suitable substrate materials that can withstand such temperature extremes, and to ensure the proper cooling. Blasting procedures to roughen the surface (generally materials having a surface hardness of about 55 HRC or lower) is also an integral part of thermal spray processes. This activates the surface by increasing the free surface energy and also increases the total surface area for bonding of the sprayed particles. Special processing techniques are required to prepare substrates with higher hardnesses [5].

In terms of the coating material, almost any material that does not decompose while being melted can be used. This includes a variety of materials, such as metals, ceramics, cermets and even some polymers - this means a nearly unlimited number of combinations [5]. However, it is necessary to assume that physical characteristics, such as coefficient of expansion, density, heat conductivity and melting point, or additional attributes, such as particle shape, particle size distribution and manufacturing process of coating material will influence the coating's properties and performance.[15][16][17].

The advantage of thermal spray technology is undoubtedly the ability to apply coatings from materials with a high melting point, such as tungsten or technical ceramics. Compared to other technologies, it also has the widest operating temperature range and coating's thicknesses. It is thus possible to apply layers with a thickness in the order of tens of μm up to several mm. The evident disadvantage is the possibility to coat only the visible surfaces of the components [5].

2.2.1 Selected thermal spray technologies

Thermal spray methods are constantly evolving depending on market developments and pressures caused by price competitiveness, regulations on products and materials, or requirements for environmental protection, health and safety [18].

In principle, the individual processes (selected ones are compared in Table 1) differ from each other by the temperatures reached during the process, which allows to apply different materials under different conditions. They also vary in the in-flight speeds of the deposited particles. Each technology is thus characterized by a source of thermal energy, the achieved kinetic energy and the range of deposited materials [18].

Thermal spray technologies are divided according to source of the thermal energy into flame, kinetic and electrical. Flame methods include detonation spray (D-Gun), flame spray, high-velocity oxy-fuel spray (HVOF) or high velocity air fuel spray (HVAF). The

technology using a kinetic method is cold spray and the electric ones include, for example, wire arc spray or plasma spray [18].

Table 1: Comparison of selected thermal spray processes [19]

Attribute	**Flame spray**	**HVOF**	**Wire arc**	**WSP-H**	**RF-ICP**
Power input [kW]	20	150-300	2-5	80-200	40-200
Jet temperature [K]	3500	5500	>5000	>25000	>10000
Particle temperature [°C]	2500	3300	>3800	>3800	>3800
Particle velocity [m/s]	50-100	200-1000	50-100	50-150	20-50
Feedrate [g/min]	30-50	15-50	150-2000	>2000	20-50
Typical thickness [mm]	0.2-10	0.1-0.3	0.2-10	0.2-10	0.05-1
Density [%]	85-90	>95	80-95	85-95	95-99
Occurrence of oxides	high	moderate to high	moderate to high	moderate to high	none

Flame spray (shown in Fig. 2.4) is probably the oldest thermal spraying process. The coating material can be fed in a form of powder, wire or rod. Flame spray technology uses a reaction of combustible gas (usually acetylene, propane, hydrogen or methylacetylene-propadiene propane (MAPP) gas) and oxygen to melt the coating material by the produced flame and carry it to the surface of the substrate. The in-flight speeds of particles are not very high (usually <100 m/s) and the bond strength of the coatings is generally also lower than for the higher speed processes. The main advantage is low capital investment, high deposition rates and ease of use (components are often sprayed manually). The disadvantage is the higher porosity and significant heating of the substrate. In wire flame spraying, the main difference is in the melting of a wire rather than powder by the flame and the subsequent atomization of the molten material by the gas stream [5][20][21].

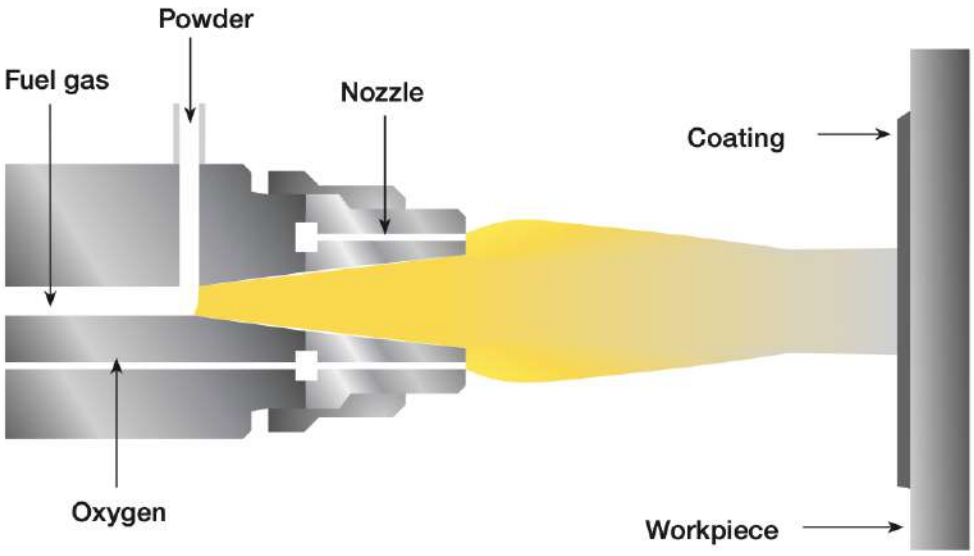

Figure 2.4: Scheme of (powder) flame spray technology [5]

High-velocity oxygen fuel spray (HVOF) is, in principle, a high-speed flame spray (Fig. 2.5) that uses high-pressure, oxy-fuel combustion (combination of oxygen with hydrogen, propane, propylene or even kerosene). The combustion takes place in a high-pressure chamber and the gases exit through a small-diameter nozzle. Thereby, a supersonic gas stream with a very high velocity of entrained particles is generated. The result are coatings with higher density and cohesiveness than from common flame sprays, but at a higher process costs [21]. The achievable particle temperatures are between 2500 °C and 3200 °C. The coating material in a powder form is injected into the stream, heated and accelerated towards the substrate. The particles bond tightly and produce a dense layer with very good adhesive and cohesive properties [22].

Dense coatings with low amount of degradation, oxidation and phase transformation due to relatively low temperature of flame are the main advantage of the technology [22]. Recently, **cold spray** technology, which is a kind of successor to HVOF, has found its applications. The kinetic energy is increased while the thermal energy is lowered. With cold spray, it is possible to eventually spray oxide-free coatings [23].

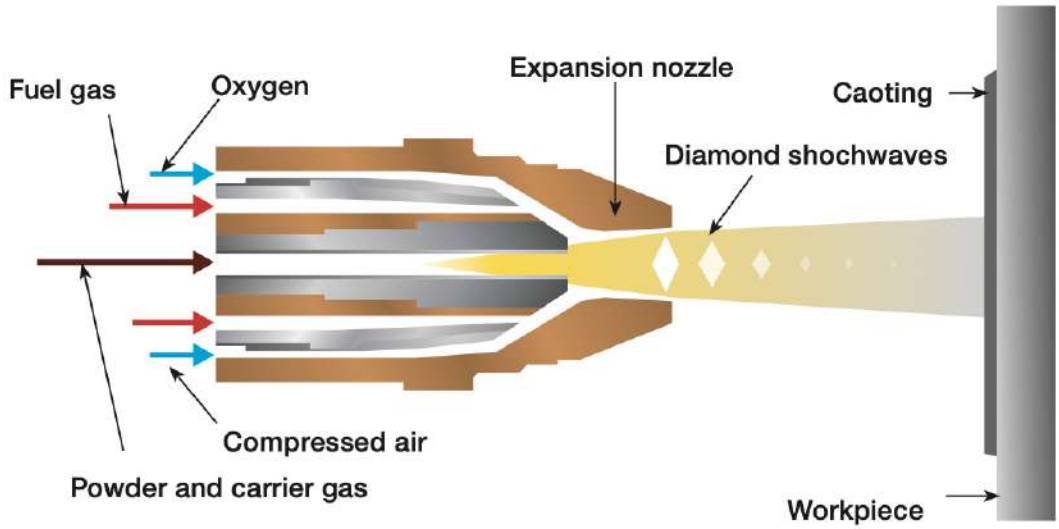

Figure 2.5: Scheme of HVOF technology [5]

Electric arc spray (sometimes referred to as wire arc spray) is a process where two consumable wire electrodes are continuously fed into the gun and an electric arc is created between them, which melts their ends. The molten material from the electrodes is atomized and entrained by a gas (most often air) stream flowing towards the substrate, where it solidifies in a form of a dense coating. This process (as shown in Fig. 2.6) has a high energy efficiency - most of the input energy is used directly to melt the material (the electrodes) while keeping the substrate temperature low because there is no hot jet of gas. Thus damage, metallurgical changes and distortion of the substrate material can be effectively avoided. Electric arc sprayed coatings are denser and stronger than flame sprayed coatings. Low running costs, as well as high spray rates and efficiency make it profitable for spraying large areas and high production rates. The disadvantage of the process is the limitation of spraying of electrically conductive materials only. Also, if substrate preheating is needed, a separate heating source is required [20][21][24].

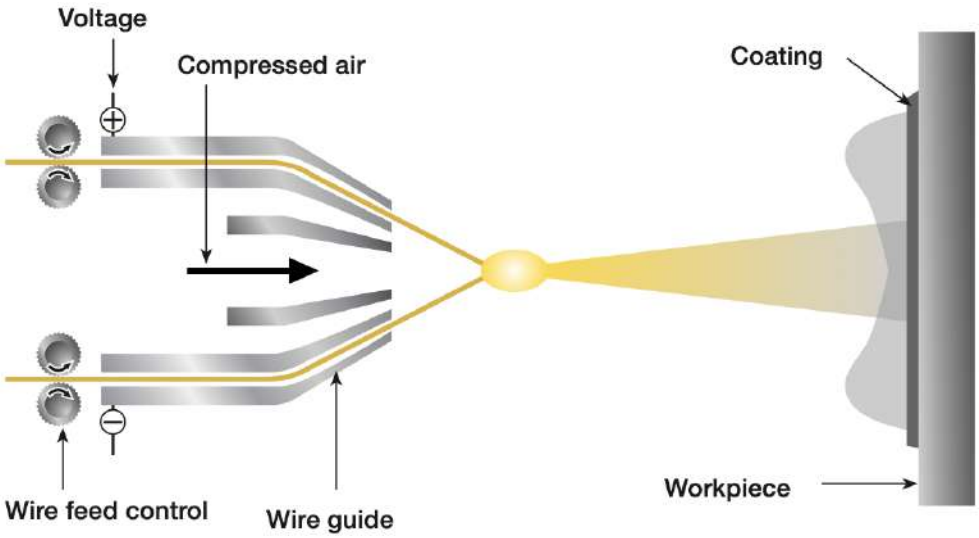

Figure 2.6: Scheme of electric arc spray technology [5]

Plasma spray uses a plasma stream as a source of thermal energy to melt and transport the coating material towards the substrate. Generally, a plasma is an electrically charged gas composed of electrons, ions, neutral atoms and molecules. It can also be defined as an ionized, macroscopically neutral gas in which free electrons and ions exhibit collective behavior. Because the particles in plasma have an electrical charge, the motion and behavior of plasma is affected by electrical and magnetic fields. This is the main difference between gas and plasma. Plasma is mostly created when extra energy is added to a gas. High temperatures often cause plasma to form. Also high energy photons, from gamma rays or X-rays or ultraviolet radiation, can create plasma. The most industrially used plasma-forming option is the high voltage electricity, where both direct current (e.g., APS, WSP-H) and alternating current (e.g., RF-ICP, microwave plasma) can be used. Table 2 gives a frequency classification for the various types of common plasma sources used in coatings deposition [25][26][27].

Table 2: Frequency range for plasma sources [26]

Type	**Frequency range [MHz]**
DC, low-frequency	<1
Radio-frequency	1-500
Microwave	500-10000

What distinguishes plasma spray from other coating technologies are its high deposition rates and ability to apply a wide range of materials. Since the temperatures in the plasma stream are normally in the range of 10000–15000 °C, it is thus possible to deposit even refractory materials such as ceramics or tungsten. The coating material can be introduced into plasma stream in the form of powder, wire, or rod. Molten particles of the coating material are then entrained to substrate's surface where they solidify and form the typical splat structure. In air plasma spraying (APS, principle shown in Fig. 2.7), the splats have a thickness of few micrometers and a diameter ranging from 10-100 μm. Usually, the minimum thickness to form a consistent coating is about 50 μm [26][27][28].

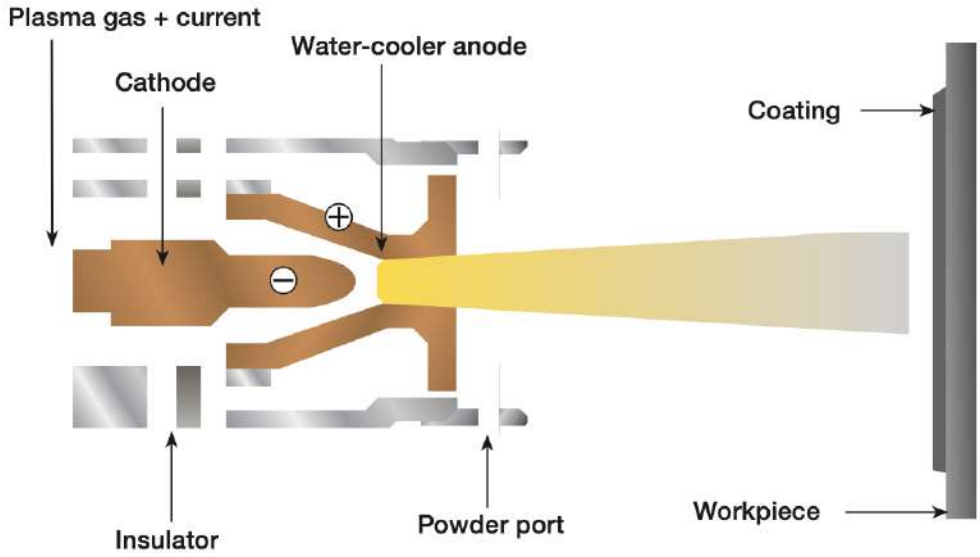

Figure 2.7: Scheme of atmospheric plasma spray technology [5]

The disadvantage of this high-temperature process is that a large amount of oxide inclusions are usually formed during the deposition. Therefore, plasma spraying under reduced pressure (e.g., vacuum plasma spray) has been developed to obtain coatings without those defects [21][29]. In fact, plasma spray technologies can be classified according to the environment where the process is performed. These include [30]:

- Atmospheric plasma spray (APS) or hybrid water-stabilized plasma spray (WSP-H) - air atmosphere
- Vacuum plasma spray (VPS) or low pressure plasma spray (LPPS) - spraying is realized in a protective chamber at low pressure or in vacuum
- Controlled atmosphere plasma spray (CAPS) or Inert Plasma Spray (IPS) - chamber contains inert gas, usually Ar, He or N_2

Radio frequency inductively-coupled plasma (RF-ICP) technology is a special type of plasma spray realized in vacuum or in the inert atmosphere. Since this technology was used to deposit bioceramic coatings in the experimental part of this thesis, it will be discussed in more detail in its own section 2.3.

2.3 Radio frequency inductively-coupled plasma

This technology belongs to the group of plasma spray processes using alternating current to create the plasma. Electric current sources are often driven at frequencies in the range of 1-200 MHz, i.e., within the radio frequency (RF) domain. In particular, 13.56 MHz and its harmonics are popular choices as they are set aside for industrial, scientific and medical applications (ISM band) [26].

Generally, the plasma torch of RF-ICP is a tube that is placed inside an induction coil. This tube is open on one side and the plasma is maintained by the passage of gases. The function of the ceramic tube is to isolate the plasma from the induction coil

and to direct the flow of the plasma gas. The induction coil is internally cooled with water. The source of high frequency current flowing through the coil is a radio frequency generator. The high-frequency current generates an oscillating electromagnetic field with an intensity vector parallel to the axis of the plasma torch. Free electrons are formed in the outflowing gas after the ignition. It is necessary to supply energy constantly to the free electrons to maintain the plasma discharge. The electrons acquire sufficient kinetic energy by acceleration with electromagnetic field and cause avalanche ionization of the gas, creating a discharge. The plasma discharge reaches temperatures from 5000 K to 10 000 K, and thus the plasma is able to ionize most elements. It is necessary for the external plasma gas to reach at least a certain critical flow rate at a given power input to the plasma to ensure the stability of the discharge. The scheme of RF-ICP technology is shown in the Fig. 2.8 [26][31].

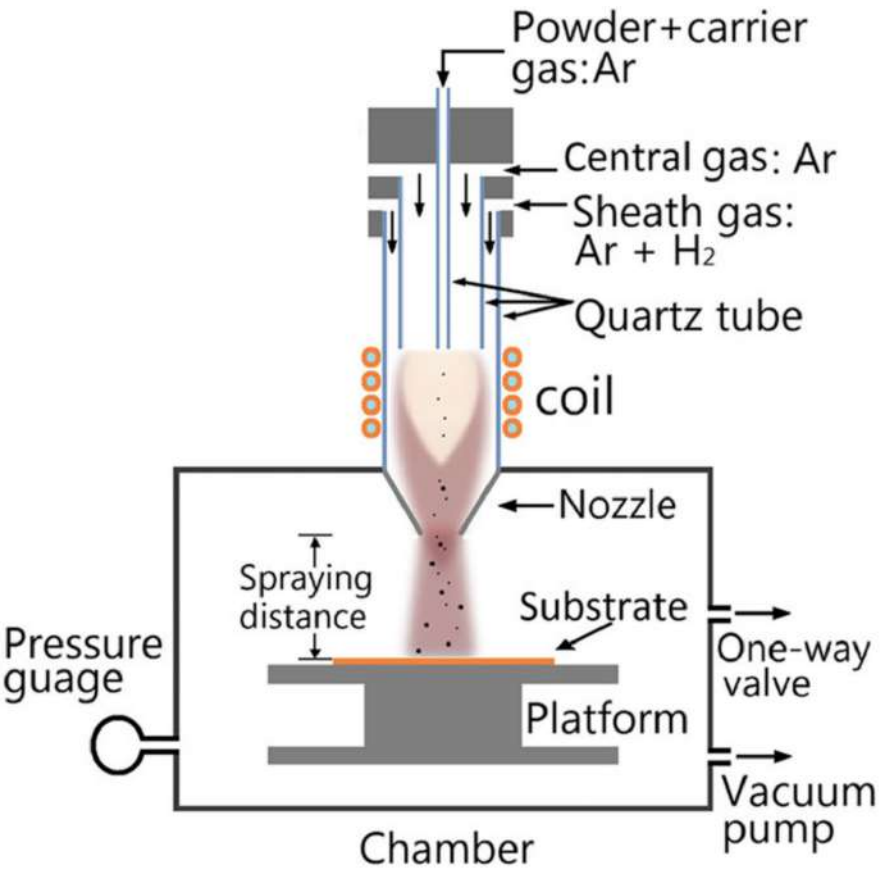

Figure 2.8: Scheme of radio frequency inductively-coupled plasma technology [32]

Monoatomic gases are most suitable to use for plasma generation as they produce simple spectra, do not form stable compounds, and have high ionization energy, thereby allowing efficient ionization. The most commonly used are Ar and He. In terms of ionization energy and thermal conductivity, He is better than Ar, however, when He only is used, it is difficult to initiate a discharge. Also, operating costs of He are higher, therefore Ar is used more often. In addition, the slightly worse Ar properties can be compensated by the addition of H_2 or N_2 [33].

2.3.1 RF-ICP applications

Radio frequency inductively-coupled plasma has many practical applications, such as determination of chemical compositions (ICP-AES and ICP-MS), etching (ICP-RIE), powder spheroidization or nanoatomization, or coating deposition. All these most common uses of RF-ICP will be described in more detail in the following text.

ICP-AES - Inductively-coupled plasma - atomic emission spectrometry, also referred to as inductively-coupled plasma optical emission spectrometry (ICP-OES), is an analytical method used to determine the content of concentrations of individual elements in the analyzed sample at levels from 1 to 10 particles per billion (ppb). The principle of this method (Fig. 2.9) lies in a spontaneous emission of photons from excited atoms and ions using the inductively-coupled plasma as the excitation source. Argon plasma operates at atmospheric pressure and is kept by inductive coupling to a radio frequency so that the standard frequency of operation is 27.17 MHz or, less commonly, 40.68 MHz. The resulting plasma reaches temperatures of about 10 000 K. The sample, in a liquid, solid, or gas form is transferred to the plasma which creates free atoms with electrons excited to higher energy levels by the energy of the plasma. Since the excited state is not stable, it is immediately deexcited to lower, more stable energy states, emitting photons of a defined wavelength, determined by the energy difference between the levels. Individual wavelengths are characteristic of given elements and the total number of photons is equal to the concentration of the elements contained in the sample. In practice, favorable analytical results are obtained for approximately 70 elements, with detection limits usually reaching the ppb level [34].

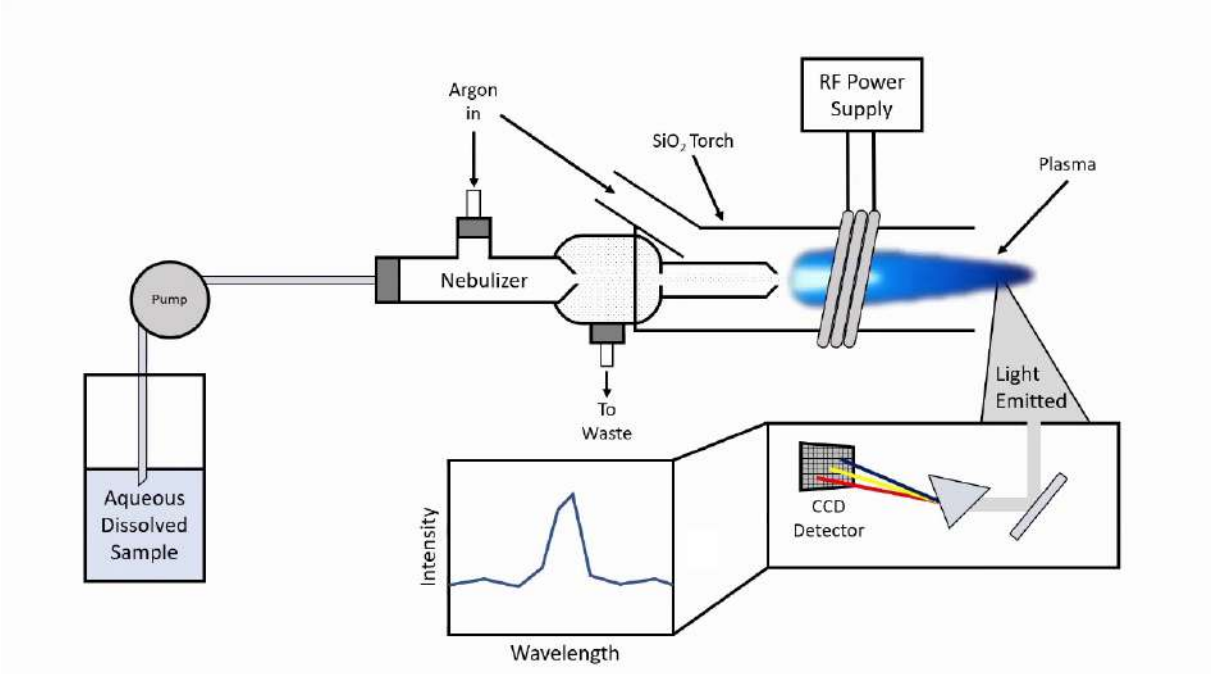

Figure 2.9: Scheme of ICP-AES device [35]

ICP-MS - Inductively-coupled plasma - mass spectrometry (Fig. 2.10) is an analytical method combining inductively-coupled plasma and mass spectrometry to determine low concentrations (ppb = parts per billion) and ultra-low concentrations of elements (ppt = parts per trillion). As with optical emission spectrometry, the sample is first transferred to a solution, then passed through a stream of argon into a plasma torch and injected into the plasma. The solvent is immediately evaporated and free atoms are formed in the gaseous state. A large group of elements has a first ionization potential lower than Ar and forms positively charged ions in the plasma. Elements such as fluorine or noble gases cannot be ionized and measured in this environment [36][37].

The advantages of ICP-MS are extremely low limits of detection (up to three orders of magnitude lower than ICP-AES) available for almost all elements of the periodic table, i.e., the possibility to analyze almost all elements. Further advantages include the ability to detect isotope composition of elements. The disadvantages and weaknesses of the ICP-MS detection, on the other hand, are the occurrence of spectral and non-spectral interferences and the high costs [36][38].

The ICP-MS method is used in all areas of elemental analysis - from water analysis, through metallurgy, geology, nuclear industry, environmental samples analysis, to biological applications [38].

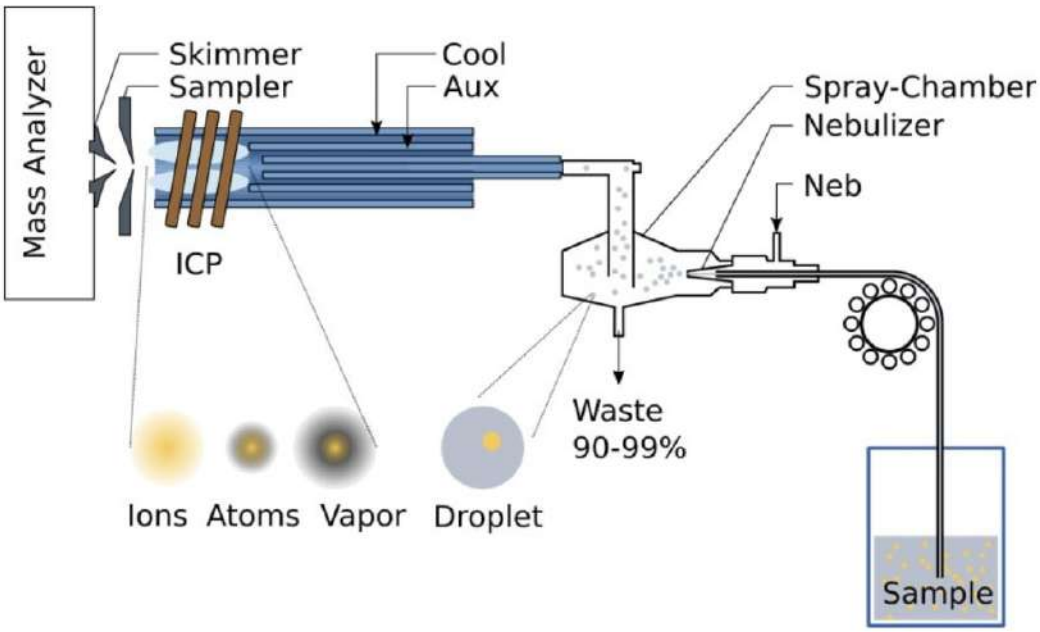

Figure 2.10: Scheme of ICP-MS device [39]

ICP-RIE is a reactive-ion etching method using inductively-coupled plasma. Plasma etching is conditioned by the generation of the ions and directing them at the substrate. Once the ions reach their target, they can mechanically or chemically remove atoms from the substrate. The ICP-RIE, shown in Fig. 2.11, consists of two generators - ICP generator as an energy source and capacitively coupled plasma (CCP) generator placed in table with the substrate. The ICP produces a magnetic field which induces an electric field directing the plasma stream towards the substrate. The CCP provides the plate bias

and causes the vertical alignment of ions and radicals in the plasma. This extension of RIE technology allows almost independent control of energy, which leads to independent control of the number of ions reaching the substrate causing chemical etching using ICP, while CCP controls the momentum of the ions reaching the substrate to mechanically etch. The ICP-RIE technology compared with RIE provides higher etching rate, better uniformity, higher selectivity and also lower crystal lattice damage [40][41][42][43].

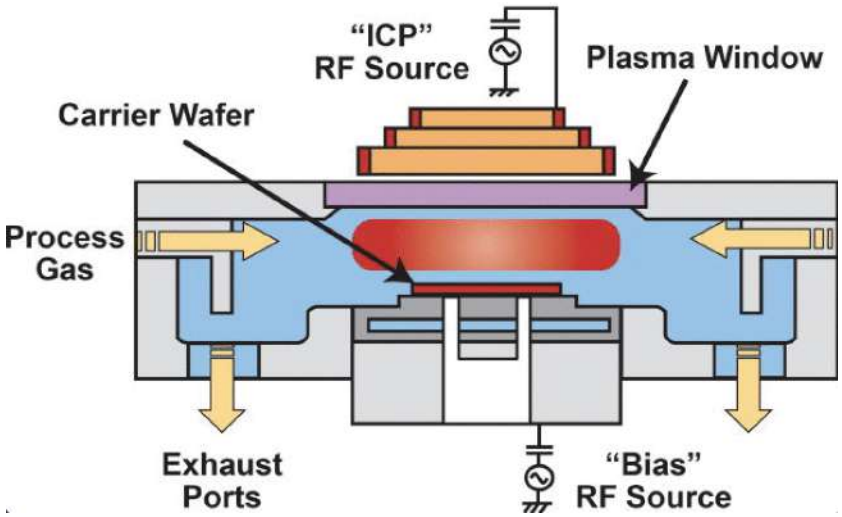

Figure 2.11: Scheme of ICP-RIE device [44]

Powder spheroidization and nanoatomization can also be achieved using the plasma spray processes. Among the various kinds of plasma technologies, RF-ICP has advantages of large volume, ultra-low contaminant levels, high energy levels, and negligible chemical reactivity since it is produced without electrodes and in a protective atmosphere (unlike DC plasma). Furthermore, the particles reaction occurs due to relatively long time spent in plasma stream as a result of the low plasma velocity (<50 m/s) [45].

In terms of spheroidization (process shown in Fig. 2.12), the powder particles in angular form are carried by a gas stream and fed axially into the plasma torch zone. The high temperature in the plasma torch zone cause the particles to melt and form liquid droplets of spherical shape under the action of surface tension. Flying out from the plasma torch zone, the droplets rapidly solidify. Finally, the spherical shape powder particles are collected at the bottom of the cooled chamber [46].

If needed, the injected particles may be exposed to not only spheroidization by melting, but also to size reduction by partial evaporation. The size reduction is strongly dependent on the initial sizes of the injected particles [47].

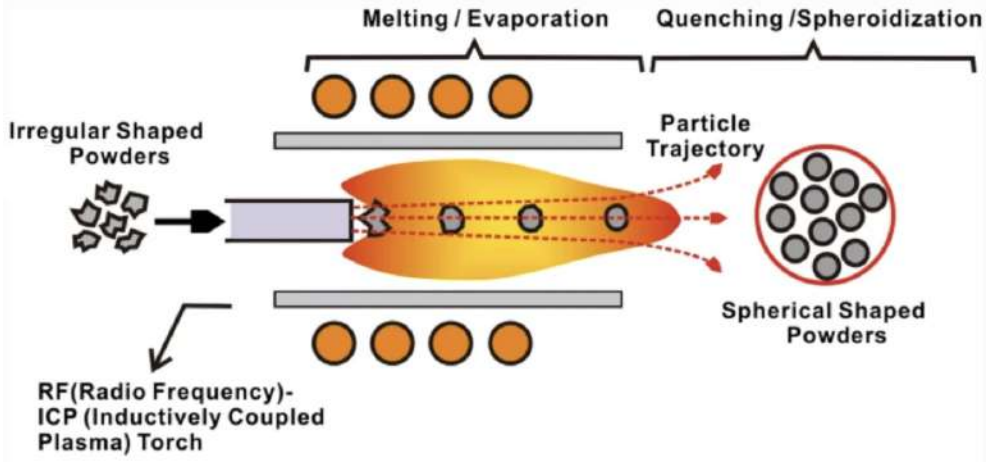

Figure 2.12: Description of powder spheroidization process [47]

Powder nanoatomization proceeds slightly differently. The principle is to inject the material into a plasma torch zone, where this material is melted. Subsequently, the molten particles are entrained by a gas stream into a chamber, where they rotate and gradually cool down. During the rotation, droplets are dispersed and form very small droplets and gradually cool down in the chamber and finally fall into the collecting filters [48].

Coating deposition using RF-ICP, mentioned in section 2.3 (principle is shown in Fig. 2.8), is the technology used in the experimental part of this thesis. The coating material is injected into the plasma stream, where molten particles are formed at high temperatures. These particles are accelerated by the gas towards the surface of the substrate and thus solid coatings are formed having structures similar to other thermal spray technologies (i.e., composed of individual splats). The deposition takes place in a sealed environment, and since this method does not include electrodes, it is possible to use, beside inert gases and vacuum, also active gases (such as CO_2), which would otherwise damage the DC plasma spray electrodes. Owing to the sealed environment, the materials are not further oxidized, which is why this method is suitable for coating of sensitive materials. Simultaneously, high deposition efficiency is the advantage of this technology. On the other hand, the overheating of the substrate and related need of significant cooling of the device may be the weakness of the process [21][29][31].

2.4 Biomaterials

Biomaterials are inanimate materials designed to interact with a biological system. They are used as a replacement for a part of living tissue or for a close contact with the tissue when the part of the body lacks its functionality due to illness or injury [49].

Biomaterials are also used to aid in healing, to improve performance, or to correct body abnormalities. Ongoing research and development of biomaterials has given rise to a separate field, tissue engineering, and currently makes it possible to replace essential parts of the human body, such as bones, joints, arteries, eye lenses and even heart valves, as illustrated in Fig. 2.13 [50][51].

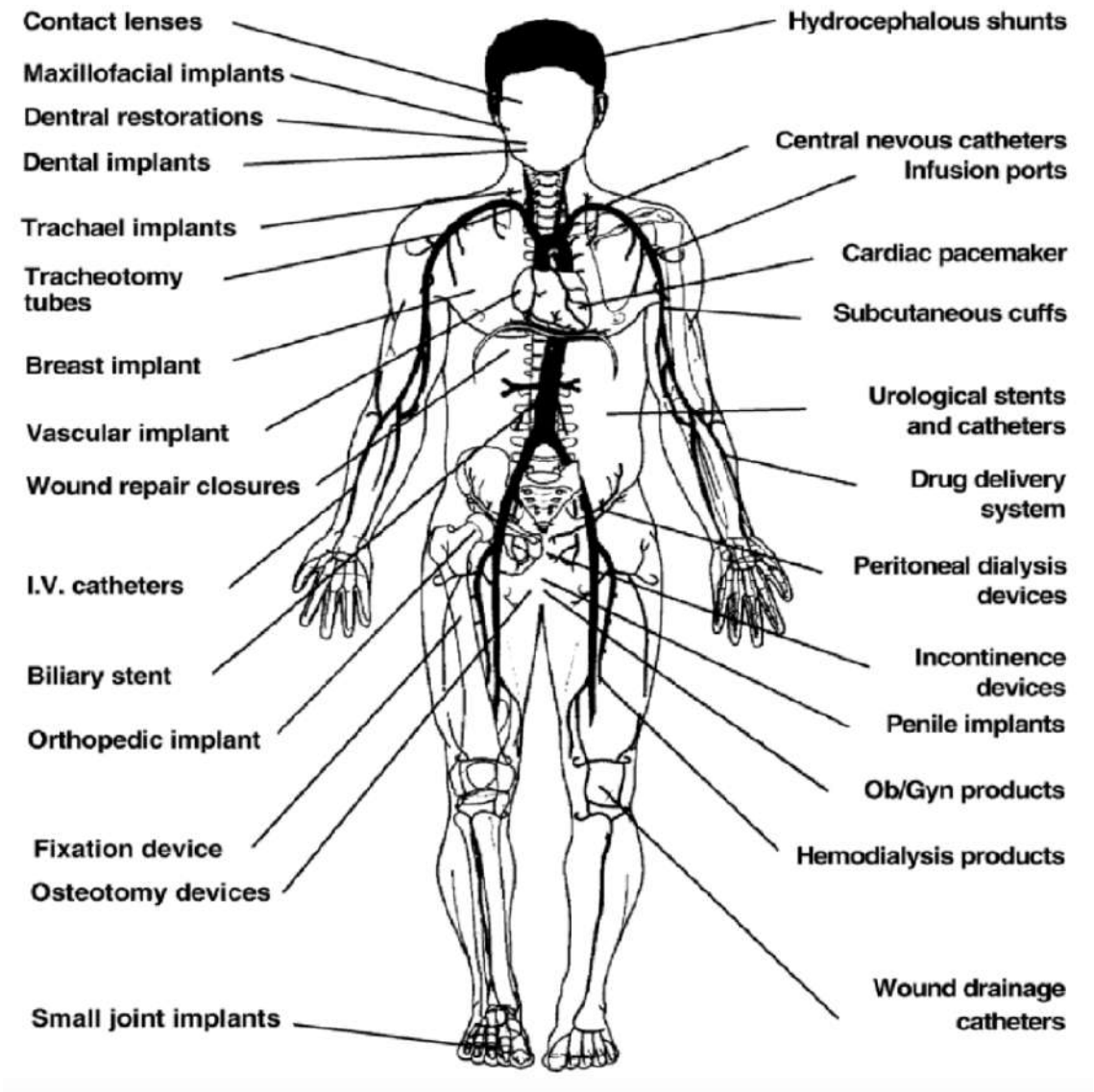

Figure 2.13: Illustration of various implants used to replace or enhance damaged tissue [51]

Materials in relation to bioapplication are divided into different classes according to their ability to remain in organism without damaging the environment or interrupting the healing process. They can be divided as follows [52][53]:

- **Biotoxic materials** - pathogenic and atrophic changes or total rejection of living tissue due to chemical processes that occur in interaction with the organism. These materials most often include alloys containing cadmium, vanadium or other toxic elements, carbon steels or methyl-methacrylate.
- **Bioinert materials** are biologically inactive and do not cause any undesirable changes in the organism. However, the presence of bioinert implant causes a formation of non-adherent fibrous capsule during the healing process to isolate host from the implant. These materials include, for instance, tantalum, titanium, aluminum, and zirconium oxides.

- **Bioactive materials** are biologically active, form direct biochemical bonds between their surface and the tissue and support its growth. These materials include calcium phosphate ceramics, some types of bioglasses, or bioactive titanium.

- **Biodegradable materials** gradually degrade in the organism and new tissue is formed in their place. This includes materials such as porous hydroxylapatite, some types of bioglass, magnesium and zinc or their alloys.

Representatives of biomaterials can be found in polymers, metals and, of course, in ceramics [49].

Synthetic polymers, such as PEG, PLGA, PMMA and others find applications in particular in soft tissue replacements ranging from facial prostheses through tracheal tubes to contact lenses. Other applications can be found in medical adhesives and sealants [54]. In addition, natural polymers, such as collagen, fibrinogen, hyaluronic acid or elastin, are also biomaterials used in soft tissues due to the presence of specific amino-acid sequences in them that cells can recognize [55].

Metal-based biomedical replacements, such as stainless steels, Ti or Co based-alloys, are widely used due to their inert nature and structural and mechanical properties. They are used for bone restorations and joint prostheses (hips, knees, shoulders and ankles) [56][57].

Ceramics are materials often used for repairing or replacing damaged bone tissue. In general, ceramics are not cytotoxic and, in addition, some types can directly bond with bone tissue. Depending on the application, the ceramics can be used as a dental prosthesis, a bioactive coating for a steel implant, but also as a self-supporting scaffold for the formation of new bone tissue [54][58][59].

However, biomaterials often require further processing, chemical treatments, and other adjusting technologies to prepare biocompatible components. The surface of the selected biomaterial comes into contact with the human tissue. Therefore, it is crucial that no toxicity or any undesirable effect, such as defensive immunogenic response, is caused by the surface. Response of the organism depends on a several factors such as contact duration, morphology, degradation rate, porosity, shape, size and sterility [56].

For instance, bone implants tend to be more susceptible to biological corrosion causing a possible release of undesirable metallic ions (such as Ni, Co and Cr) from the implants that could result in allergic reactions [60]. Nevertheless, this does not apply to Ti6Al4V alloy used for bone or dental implants. This Ti-based alloy has its native oxide layer that exhibits electrochemical inertness. However, in regions interfacing the soft tissue, its surface may be exposed to microbial actions leading to infections. In addition, it has been estimated that up to 80% of the infections in hospitals are caused by bacterial formations on the surfaces of biomaterials, implants or surgical devices. The potential risks and consequences of exposure of the implant to living tissue are shown in Fig. 2.14 [56].

Therefore, surface treatments of implants, especially coatings deposition, have been investigated to suppress such risks. Often, natural polymers such as chitosan, dextran, alginate, and hyaluroran are used to coat the implants due to their bioactivity and sometimes anti-microbial properties. In case of ceramic biomaterials, in particular hydroxylapatite coatings shown to be very effective in supporting cell growth and osteointegration [56][61].

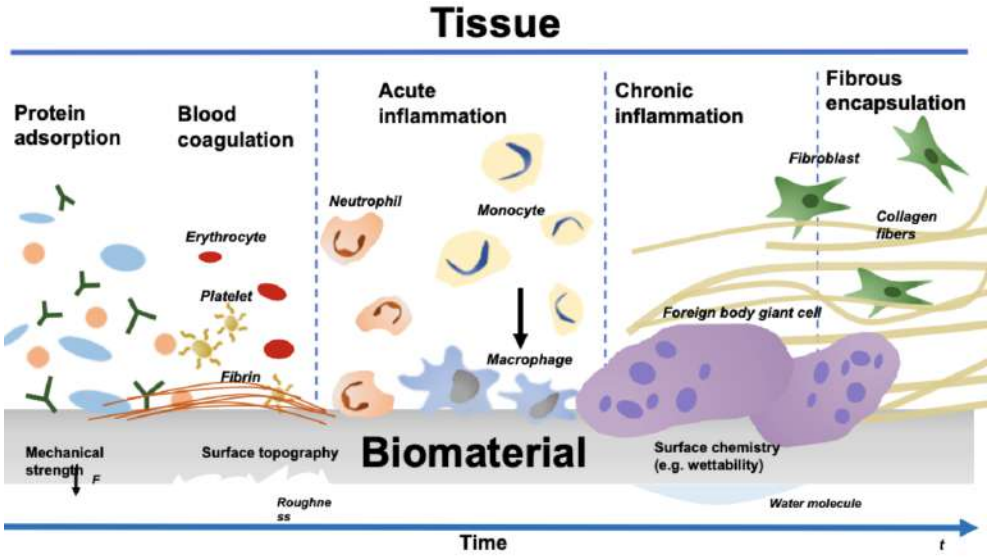

Figure 2.14: Schematic representation of human organism response to implanted biomaterial [56]

2.5 Metal-based biomaterials

Musculoskeletal disorders cause pain in the joints, muscles and tendons, and worsen the condition of the tissues. These disorders affect the lives of millions of people, and it is estimated that these disorders will increase in numbers due to today's lifestyle. A study by Kurtz et al. estimates that between 2005 and 2030 in the USA alone, over 570,000 hip replacement and about 3.5 million knee replacement procedures should be performed [62]. Musculoskeletal problems are most often solved by surgery, and in the case of a joint replacement, metal-based biomaterials play a crucial role. Table 3 shows a comparison of tensile strength, yield strength and Young's modulus of the most commonly used metallic biomaterials along with corresponding values of a cortical bone [53].

Table 3: Comparison of physical and mechanical properties of various implant materials with natural bone [63][64][65]

Material	ρ $[g/cm^3]$	R_m [MPa]	R_e [MPa]	E [GPa]
Cortical bone	1.80-2.10	70-150	30-70	15-30
Stainless steel	7.90-8.10	490-1350	190-690	200-210
Co-Cr alloys	8.30-9.20	655-1793	310-1586	210-253
Ti-based alloys	4.40-4.50	690-1100	585-1060	55-110

As illustrated in Table 3, the leading metallic biomaterials for orthopedic and dental applications include stainless steel, as well as Co-Cr-based and Ti-based alloys. All these materials differ in their mechanical properties and each of them finds its application according to the requirements. The implant materials have made a great progress over the years, but there are still niches for improvement. In the long run, these materials can fail for a variety of reasons, such as corrosion, wear, low strength or mismatch of Young's modulus with the body parts. The mismatch of the Young's modulus is one of the specific problems associated with the application of biomaterial as a bone implant. Under normal conditions, the bone carries the entire load itself. However, after implant application, the load is distributed between the implant and the bone. This is called stress shielding. When the bone is less stressed, its mass decreases. This loss of bone mass is referred to as bone resorption and can cause the implant to collapse. In this respect, the lower-modulus titanium alloys are currently the number one choice for orthopedic applications and will therefore be described in more detail in section 2.5.1 [53][66].

2.5.1 Ti and Ti-based alloys

Titanium exists in two allotropic forms - α and β. At room temperature, titanium is formed by the α-phase, which has a hexagonal close-packed (HCP) structure, while, when the temperature exceeds 883 °C, β-phase is formed, which has a body centered-cubic (BCC) lattice [53].

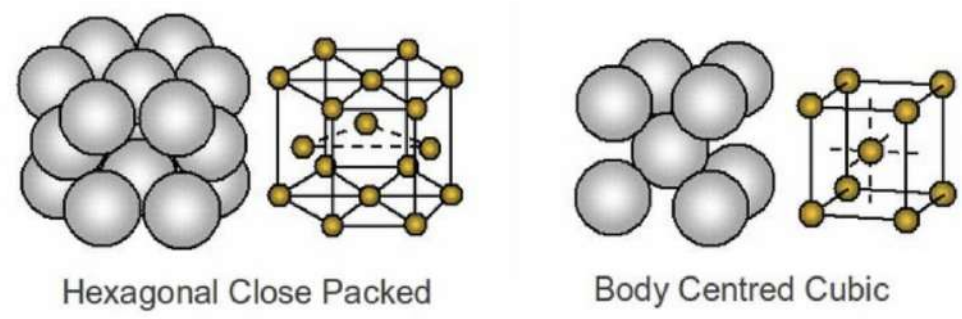

Figure 2.15: HCP structure of α-Ti (left) and BCC structure of β-Ti (right) [67]

Titanium is a metal that is used in many fields due to the fact that its composition can be easily changed by adding suitable alloying elements. Titanium alloys form five categories according to the content of Ti phases - α, near α, α+β, near β, β. Near α-phase is similar to α-phase at low temperature, however, 5-10% of β-phase forms during the heating. α+β contains most of the α-phase and the transformed β-phase makes up the rest, usually 10-30%. Near β-phase retains β-phase near the transformation temperature during initial cooling, but upon heating, secondary phases begin to precipitate [53].

Various elements are used to stabilize the desired phases, divided according to whether they stabilize the α-phase or the β-phase. The α-phase stabilizing elements include Al, O, N and C. These elements increase the temperature at which the phase is stable, while β-stabilizers decrease the temperature at which the β-phase is stable. These β-stabilizers include V, Nb, Mo and Ta. The influence of these elements can be observed, for instance, in the phase diagram of the Ti6Al4V alloy in Fig. 2.16. Each Ti-based alloy has a tem-

perature called β transus. This temperature is very important because the necessary heat treatment is performed close to this temperature. Needless to say, the choice of the processing temperature is important because it controls the stabilization of the various phases and, in turn, their content affects the mechanical and other properties of the final titanium alloy [53].

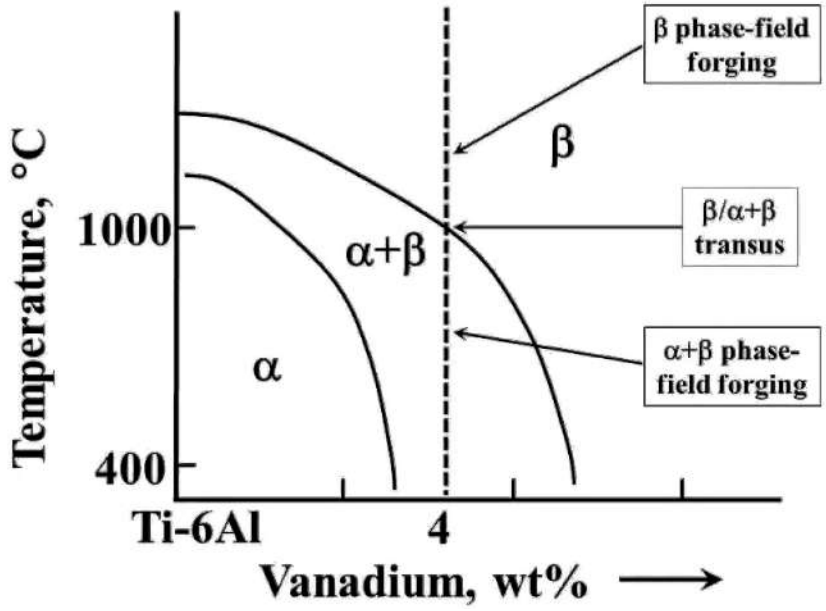

Figure 2.16: Ti6Al4V phase diagram [68]

Endoprostheses were originally made of stainless steels such as AISI 316L or AISI 304. Alloys based on Co-Cr-Mo were also used, but the applications gradually moved to Ti-based alloys which show bioinertness combined with suitable mechanical properties. The α+β alloys, such as Ti6Al4V and Ti6Al4V ELI (extra low interstitial content), are the most widely used alloys for orthopedic applications; however, their use has certain limitations. For this reason, the research has focused on the development of β alloys, as they show better biocompatibility and even lower Young's modulus. At the same time, it has been found that if vanadium is released into the body, it can be cytotoxic. For this reason, research has begun on β-Ti alloys stabilized with elements other than V. Ti6Al7Nb and Ti5Al2,5Fe appear to be promising candidates so far. Both alloys show similar strength, but higher ductility and corrosion resistance [53][69].

2.6 Bioceramics

Throughout the history, various attempts have aimed to replace hard tissue with biomaterials and to restore physiological functions caused by injury or disease. In this respect, various types of materials have proved to be useful, but ceramics have received attention due to their exceptional properties, such as chemical resistance, tensile strength and wear resistance. Moreover, in the 1920s, the first similarities between bone material and calcium phosphate compounds, specifically hydroxylapatite (HA), were discovered. Thus after 1960 came the era of research of ceramics for bioapplications [70].

In these days, bioceramic replacements, as they can be manufactured in porous or in dense form, are used in many different applications throughout the body. According to the interaction between the bioceramic implant and the living tissue, they can be defined and categorized as bioinert or bioactive, while bioactive ceramics may also be resorbable in the body [70]. These categories are described as follows:

- **Bioinert ceramics** are the earliest ceramics used to repair damaged part of tissue in order to elicit minimal biological response from the physiological environment. In the other words, they are tolerated by the living tissue. The bone tissue is not chemically bonded to the implant, thus the bone cells can only colonize the surface. In the case of porous ceramics, the newly formed bone tissue penetrates the pores for a short distance. However, usually during the healing process a connective tissue forms around the implant as the organism's reaction to the presence of a foreign body [70][71]. The most commonly used bioinert ceramics are alumina and zirconia. They are abrasion resistant and hard enough, but also fragile and somewhat difficult to process. They are not soluble in body fluids and do not oxidize. For their good mechanical properties, they are mainly used for applications with high loads, such as dental and orthopedic prostheses [71][72].

- **Bioactive ceramics** have the ability to form a strong chemical bond with bone tissue directly, not through the connective tissue. In the 1970s, a glass-based ceramic material able to chemically bond not only to the bone tissue but also to soft tissue was developed. Bioactive ceramics are mainly based on hydroxylapatite, glass-ceramic materials and bioglasses. However, bioactive ceramics do not have mechanical properties as good as their bioinert counterparts, therefore they are used for applications operating under lower loads. They are often used as scaffolds or coatings for bioinert metallic bone implants. They are most useful in the porous form that bone cells (osteoblasts) can colonize and bond with. For instance, a trabecular bone is a natural composite composed of soft collagen fibers and porous bone mineral - carbon-containing apatite. This apatite makes up to 70% of the bone's hard tissue and is similar to synthetic hydroxylapatite, which is also the subject of this study and will be described in detail in section 2.6.1 [71][72][73].

- **Resorbable ceramics**, also referred to as biodegradable ceramics, are mainly used as a temporary replacement for bones. During bone regeneration, the implanted material is gradually absorbed and substituted by the bone tissue. Scaffolds are often used for this purpose. Resorbable bioceramics are usually based on calcium salts, e.g., phosphates, carbonates, or sulphates [71][72].

2.6.1 Calcium phosphate ceramic

Calcium phosphate ceramics include materials and minerals containing calcium cations (Ca^{2+}) and phosphate anions. Some calcium phosphate ceramics may contain oxides and hydroxides. These materials are used primarily in medical applications, mostly as bone and dental prostheses or as coatings for bone implants, since they show osteoconductive and in some cases osteoinductive features. The calcium and phosphorus ions have influence on the bone regeneration - they activate osteoblasts (bone-forming cells) and osteoclasts (bone-dissolving cells) which makes the bone constantly adjusted and

adapted to the load. The biological properties depend significantly on the type of calcium phosphate ceramic, which also specifies the area of applications varying depending on different ion release, solubility, stability, and mechanical strength. These differences of calcium phosphate ceramics depend mainly on their calcium/phosphate ratio and phase composition. The proportion of different phases decide whether bioactive or resorbable ceramic material is formed. The latest research focused mainly on calcium phosphate ceramics with Ca/P ratios in the range of 1.5-1.67, as they are the most interesting in terms of bioapplications [74][75][76].

Hydroxylapatite (HA) is probably the most important calcium phosphate ceramic. It occurs in nature as a mineral of different colors. HA can be found in yellow, green or most often in brown color. The synthetic HA powder in its pure form is white. As an inorganic compound, HA is a component of rocks, plants and animals. There is about 70% of HA in the bones, but most of it is in the tooth enamel, almost 90% [77][78].

The mineral part of the bone tissue is formed with a non-stoichiometric carbonated multi-substituted apatite with Ca/P ratio in the range of 1.37-1.87. The chemical formula of synthetic HA is $Ca_{10}(PO_4)_6(OH)_2$ (comprising two molecules $Ca_5(PO_4)_3OH$) and its Ca/P ratio is 1.67. As already mentioned, HA can be obtained in a natural form, but in this form, it usually possesses defective structures. Therefore, the synthetic HA is used for medical applications, which can be obtained by several synthesis methods that will be described in section 2.6.2. The stoichiometric HA can exist in both monoclinic and hexagonal lattices, but in biological system, the hexagonal lattice (shown in Fig. 2.17) is preferred due to its higher stability [75][79][80].

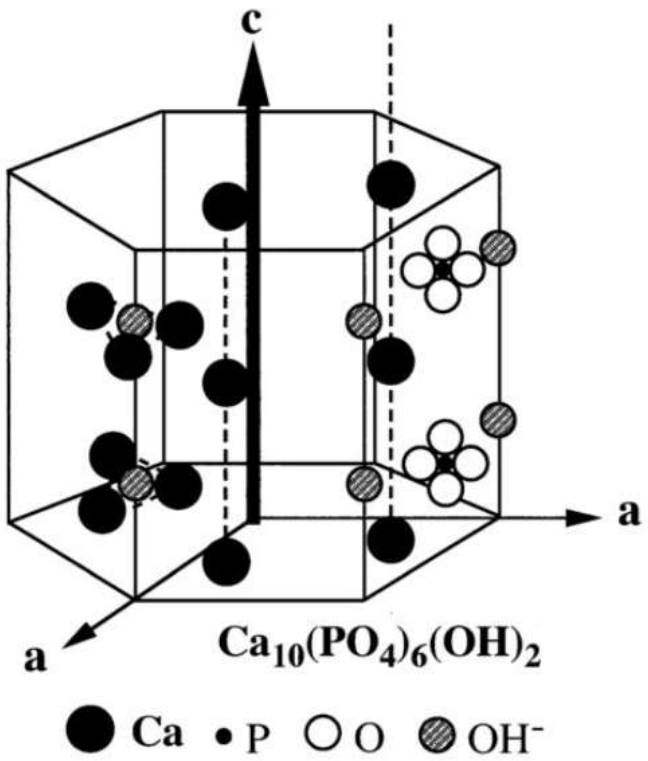

Figure 2.17: Crystal structure of hydroxylapatite [81]

Since chemical composition and structure of HA is very similar to the composition of human bones, it has been widely applied as orthopedic implants. However, the mechanical properties of 100% pure HA are not suitable for high-load applications. Therefore, HA is mostly used in composites (Fig. 2.18), or for instance as coating for metal-based implants, as self-setting bone cements, as granules for filling voids, or as larger structures [70].

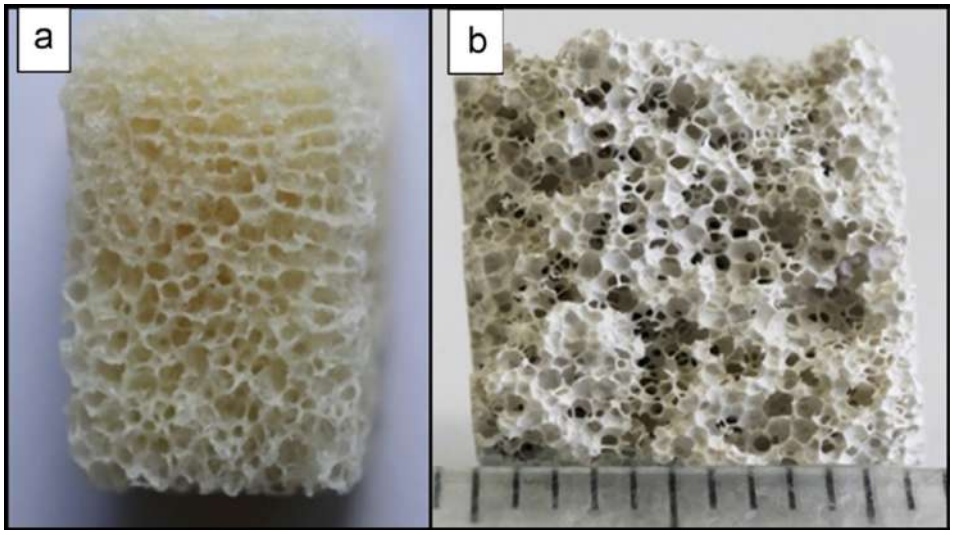

Figure 2.18: Photo of (a) human trabecular bone and (b) composite from Si_3N_4 porous ceramic coated with HA [73]

HA ceramics are used in medical applications especially for its fast and direct binding to bone tissue. They show bioactivity that creates conditions for osteoconduction and possibly osteoinduction. An analysis of implant-bone interface has shown that the presence of HA is the key for the formation of the interlayer. The interlayer starts to form on the implant's surface and is made of the cellular bone matrix from differentiated osteoblasts that produce 3-5 μm wide amorphous band where collagen appears. As the interlayer ages, the band narrows to only 0.05-0.2 μm. The result is that the implant is attached to the natural bone through a thin epitaxial layer [76][82].

Interestingly, HA began to be used as a biocompatible hip replacement instead of the previously used polymethyl methacrylate-based (PMMA) bone cement, which was shown to be responsible for the "cement disease" [83].

2.6.2 Hydroxylapatite synthesis

Since HA may be used in many different applications, it must be adapted to the conditions of use in terms of its bioactivity and mechanical properties. Consequently, the research has focused on the development of methods that allow the control of the chemical and physical characteristics of the resulting HA powder. Due to the existence of many phosphate compounds, calcium phosphate ceramics form a complex system, which is further complicated by the sensitivity of phosphates to small changes, such as composition, pH, or temperature. It is obvious that the properties of the synthesized powder can strongly influence its biological behavior. These properties thus determine the medical applications of the material. That is why several HA production methods enabling the control of, e.g., crystal morphology, chemical composition, crystallinity, particle size distribution,

or agglomeration, were developed. The following text will describe the most commonly used ones [84].

- **Wet-chemical precipitation method** may be considered as one of the most widespread methods used for HA synthesis, mainly due to its simplicity, low operative costs (low reaction temperatures) and scalability. However, the synthesis of HA entails certain inconveniences such as simultaneous occurrence of nucleation, crystal growth, coarsening and agglomeration. Reactions require optimization to ensure proper morphology and to minimize crystal growth. The precipitation method works on the basis of supersaturation of the solution (supersaturated solution is a solution containing more solutes than it should contain at equilibrium). In the case of supersaturation, nucleation and crystal growth occur, which happens when the phosphate solution is titrated into the calcium solution to form a suspension of precipitated particles. The composition of the final product depends on the temperature, pH of the solution and concentration, thus it is necessary to control these parameters to ensure the formation of a homogeneous product. The precipitated powders are subsequently calcined at temperatures of 400-600 °C to refine the crystalline structure. To sum it up, this is the most common method consisting of three steps (calcinations and sintering after processing), the disadvantage of which is difficult achievable reproducibility due to lack of precise control [84][85].

- **Hydro-thermal and solvo-thermal method** requires the use of a solvent with precursor soluble ions, which is heated in a closed vessel. In the case of the hydrothermal method, the solvent is water, while solvo-thermal method uses alcohol or any other organic or inorganic solvent. Due to the overpressure in a closed vessel, the temperature of the solvent usually exceeds the boiling point. Change in the properties of the solvent and reactants at these elevated temperatures allows wider control of the experimental variables (nucleation, crystal growth, ageing, etc.) and makes the process more predictable. The advantage of this method is undoubtedly low operation cost and short reaction time, as well as the possibility to perform the reactions at low temperatures, allowing also solid-state reactions. In addition, unlike some other methods (wet-chemical precipitation, sol-gel), this method does not require any additional heat treatment to crystallize the HA. To sum it up, this method is a single-step process capable of producing homogeneous crystal shapes and sizes. Costs depend on particle morphology. [84][85][86].

- **Solid-state reactions method** is a traditional method that is, surprisingly, only rarely used for the production of HA. The principle is a solid diffusion of ions between powdered raw materials requiring high temperature (1250 °C) to initiate the reaction. First, the raw materials must be ball milled (approximately 16 hours) to ensure sufficient particle size and homogeneity of the mixture. For that, calcium and phosphate sources are usually mixed with a binder (PVA) and additives (SiO_2, Al_2O_3, HF) to form a slurry before the ball milling proceeds. The slurry is dried afterwards. The resulting powder is then hot or cold pressed (<135 MPa) to form pellets. Finally, the powder is sintered at 1250 °C to crystallize the product. According to some references in the literature, it is recommended to crush, compact and sinter the final product again to ensure a finer-grained structure. Probably the most important reason why this method is not used for HA synthesis more often is

the fact that it is difficult to control and other calcium phosphate phases are likely to be formed during the sintering. These phases (e.g., TCP) affect the solubility and mechanical properties of the product, which is undesirable. To sum it up, the process consists of a number of necessary steps and all may be repeated several times to improve quality and reduce particle size. The reaction is slow and may result in mixed phase product [84][87].

- **Sol-gel method** has recently come to prominence due to its inherent advantages such as homogeneous molecular mixing, low processing temperature, or formation of nano-sized particles, bulk amorphous monolithic solids and thin films. However, compared to other low temperature methods, the limited scalability and high costs of the reactants make it disadvantageous. As for the principle of the method, it is first necessary to form a "sol" by dispersing the solid particles in the liquid solvent with under a controlled pH to prevent precipitation. Usually metal salts, such as $Ca(NO_3)_2$ for Ca and $(NH_4)_3PO_4$ for P, are used for the reaction. Subsequently, hydrolysis and polycondensation reactions occur, which results in a viscosity increase and the formation of a "gel". Finally, the gel is dried at 60 °C and calcined at the temperatures in range of 300-700 °C. To sum it up, the process involves more than three steps. Chemical homogeneity is improved with molecular mixing, but it is still difficult to form a single phase product [84][88].

- **Self-propagating combustion synthesis** can be used as one of the options for the production of HA as it is a simple process and saves time and energy in comparison with the other methods. A thorough mixing of the calcium and phosphate sources with the aqueous fuel (e.g., $CO(NH_2)_2$, $C_6H_8O_7$, or $C_2H_5NO_2$) and an oxidising agent (HNO_3) is an important prerequisite. By increasing the temperature of the solution, an exothermic reaction occurs between the fuel and the oxidizing agent, while the gaseous products combust. This causes the formation of a solid calcium phosphate powder. The temperatures that occur during the reaction depend on the choice of the fuel as well as on the fuel/oxidizer ratio. These parameters can be adjusted, leading to the formation of different calcium phosphate phases and morphologies. Finally, calcination must be carried out in order to crystallize the phase and to remove the organic residues. To sum it up, the reaction time of process is very short (<20 min), however, the uncontrollable high temperature of reaction is disadvantageous and may lead to mixed phases. The choice of the used fuel influences the particle morphology [84][85][89].

- **Emulsion and microemulsion method** differ in droplet size. In general, an emulsion is defined as a heterogeneous mixture of at least one immiscible liquid dispersed in the form of droplets in another liquid. Depending on the amount of one liquid in another, emulsions are often described as water-in-oil (W/O) or oil-in-water (O/W), with the O/W system being commonly used to synthesize HA. The reaction occurs when two different droplets containing reactants collide. There are references that microemulsions, compared to emulsions, are more suitable for HA synthesis because they reduce particle agglomeration. In addition, nano-sized spherical HA particles produced via microemulsion routes are suitable for plasma spraying. To sum it up, the process consists of two high temperature steps (calcination and sintering). The advantage is that the porous particles can be formed [84][90].

Table 4: Comparison of the selected HA synthesis methods [84]

Synthesis method	**Processing time [±24 hrs]**	**Reaction temperature [°C]**	**Particle size [μm]**	**Scalability**
Wet-chemical precipitation	+	20-85	>0.10	High
Hydro-/solvo-thermal	-	150-400	>0.05	Low
Solid state reactions	+	1050-1250	>2.00	Medium
Sol-gel	+	37-85	>0.001	Low
Self propagating combustion synthesis	-	170-500	>0.45	Low
Emulsion and microemulsion	+	20-50	>1.00 >0.005 (micro)	Low - medium

The methods defined above and compared in Table 4 demonstrate that there is a great variability in HA synthesis. By choosing the right method, it is possible to control the physical (particle size, morphology) and chemical (Ca/P ratio) characteristics and achieve the desired powder. Therefore, it is important to determine what properties the desired material should have and choose the method accordingly [84].

2.6.3 Plasma sprayed hydroxylapatite coatings

Plasma spray is one of the most widely used coating technologies to deposit hydroxylapatite onto metal-based implants to improve the fixation of the implant and the bone tissue growth. This is mainly due to the inherent high deposition rates and the ability to easily melt materials with a high melting point.

Figure 2.19: Hydroxylapatite coating used for a hip implant [92]

However, the associated high process temperatures and rapid cooling rates may cause physical and chemical changes in coating. The adjustment of deposition parameters such as the torch power, feedrate, or spray distance, can lead to the formation of different phase composition, crystal structure and microstructure, which may in turn result in a change of mechanical properties and solubility of the coating. This is especially significant for thin coatings. For instance, the HA coating of a femoral stem (Fig. 2.19) has a thickness usually around 50 μm [91].

Hydroxylapatite is the most stable phase of calcium phosphate ceramics in body fluids. However, since it melts incongruently, other phases may form during its plasma spray deposition. Frequently, the high temperature of the process leads to decomposition of HA to several phases, with the most common being tricalcium phosphate ($Ca_3(PO_4)_2$, TCP), tetracalcium phosphate ($Ca_4(PO_4)_2O$, TTCP), and calcium oxide (CaO). As shown in Fig. 2.20, these phases dissolve in the body fluids more rapidly than HA, in the following order: CaO > TTCP > TCP > HA [93][94][95].

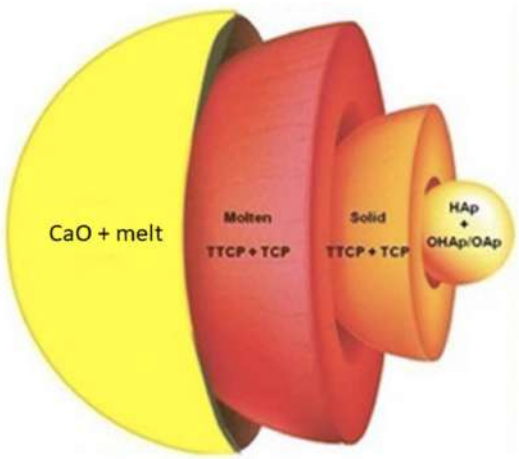

Figure 2.20: Scheme of the thermal decomposition of the hydroxylapatite particle during plasma spray process [69]

The partial content of the resorbable phases in the HA coating may actually be considered beneficial in terms of implant bioactivity because it may stimulate bone apatite formation at the implant-bone tissue interface. However, there is a risk that if the resorbable phase content is too high, the coating may deteriorate. The long-term stability of any HA coating thus depends on the occurrence of phases formed by the decomposition of HA [96][97][98].

TCP with Ca/P=1.5 generally occurs in two phases - α and β. There are differences in chemical properties and biological behavior between those two modifications. They differ mainly in their density and solubility in body fluids. The α-phase is more reactive and more soluble. This phase is usually not stable at room temperature, although it can be subsequently stabilized. It may be used for the preparation of bone cements. In HA deposition, the α-TCP is formed at high temperatures (>1250 °C) and occurs unstable. For this reason, its increased content is not desired. The β phase, on the other hand, is stable at room temperature and, owing to this, it has been used for bone replacements as one of the oldest biomaterials [99].

TTCP is a ceramic significantly depleted of phosphorus. It has Ca/P=2 which makes it the only calcium phosphate phase with a higher Ca/P ratio than stoichiometric HA. It is a metastable phase which easily decomposes into HA and CaO in the temperature range of 1000-1200 °C. Compared to other calcium phosphate ceramics that are used, e.g., as food ingredients, in tooth pastes, in pharmaceutical applications or in chromatography, TTCP only finds application as a biomaterial (as an ingredient in self-setting bone cements). However, it often occurs as an undesirable by-product in plasma sprayed HA coatings, where it is formed at temperatures above 1300 °C as a result of the thermal decomposition of HA [100][101].

Tha calcium oxide (CaO) is considered to be the fastest soluble product of calcium phosphate ceramics. Thus, the increased content in the HA coating can cause adverse effects on the stability of the coating. In addition, CaO induces an exothermic reaction that can cause burns to surrounding tissues. Therefore, its content should be reduced to a minimum [102].

Overall, apart from crystalline HA, most of the other phases are regarded as undesired. Phases such as TTCP or CaO have no proven bioactivity and moreover they dissolve faster than other calcium phosphate phases. Their presence is determined by the heating and cooling temperatures during the process. Therefore, TTCP and CaO phases should be minimized in the coating to ensure the best possible conditions for improvement of bioactivity, stability, and implant life [91][103].

3 Experimental setup

The aim of the experimental part of this work was to develop hydroxylapatite coatings on Ti6Al4V substrates using RF-ICP technology and to assess the influence of selected process parameters on the final coating's properties. This chapter will introduce the materials, methods and devices used during the experiments, as well as the characterization techniques used for the analysis of coatings' properties.

3.1 Materials

3.1.1 Substrates

Two types of commercially available substrates were selected for the experiment, stainless steel AISI 304 (Italinox, Czech Republic) and Ti6Al4V titanium alloy with purity of grade 5 (Bibus Metals, Czech Republic). The stainless steel substrates were used for optimization of the RF-ICP deposition parameters, and, based on the obtained results, the deposition on titanium alloy substrates was performed. The chemical composition of two metals is shown in Table 5 and Table 6, respectively and their material characteristics are compared in Table 7.

Table 5: Chemical composition of austenitic stainless steel AISI 304 [104]

C [%]	**Cr** [%]	**Ni** [%]	**Mn** [%]	**Si** [%]	**N** [%]	**P** [%]	**S** [%]
<0.07	17.00-19.50	8.00-10.00	<2.00	<1.00	<0.11	<0.045	<0.03

Table 6: Chemical composition of titanium alloy Ti6Al4V grade 5 [105]

Ti [%]	**Al** [%]	**V** [%]	**Fe** [%]	**O** [%]	**C** [%]	**N** [%]	**H** [%]
Balance	5.50-6.75	3.50-4.50	<0.40	<0.20	<0.08	<0.05	<0.015

Table 7: Comparison of material characteristics of AISI 304 and Ti6Al4V [104][105]

Material	ρ $[g/cm^3]$	T_M [°C]	E [GPa]	HRC	λ [W/m.K]	α [1/K]
AISI 304	8.00	1450	193	18	16.20	17.20×10^{-6}
Ti6Al4V	4.42	1650	114	36	7.20	8.60×10^{-6}

Both substrates were prepared from rolled sheets and cut to dimensions according to Fig. 3.1 with chamfered edges on the shorter sides for attachment to a dedicated RF-ICP holder. Prior to the coatings deposition, the substrates were grit-blasted and cleaned to remove impurities and residual grit by immersion in acetone and exposure to ultrasound for 10 minutes (Laboratory 2 DK120HTD).

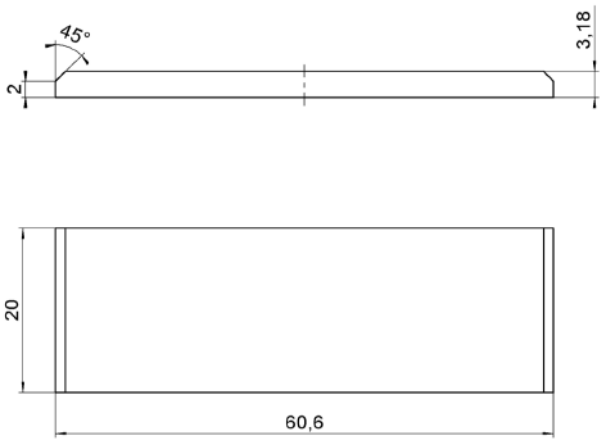

Figure 3.1: Substrate geometry used for RF-ICP deposition

3.1.2 Hydroxylapatite powder

Hydroxylapatite ($Ca_{10}(PO_4)_6(OH)_2$) powder with the particle size -150+45 μm, supplied by Medicoat, Switzerland, was used for deposition. This particular powder has been proven for a long time and is used for commercial plasma sprayed orthopedic and dental applications. The powder chemical analysis supplied by the producer is shown in Table 8, and the particles' morphology and size distribution are shown in Fig. 3.2.

Table 8: Material characteristics of the supplied HA powder [106]

Ca/P ratio	Trace elements	Heavy metals	Particle size distribution	Bulk density
1.67	Fe<34.00 ppm As<1.00 ppm Cd<1.00 ppm Pb<1.00 ppm Hg<0.05 ppm	<10 ppm	D10=60.5 μm D50=98.2 μm D90=157.9 μm	0.492 g/cm^3

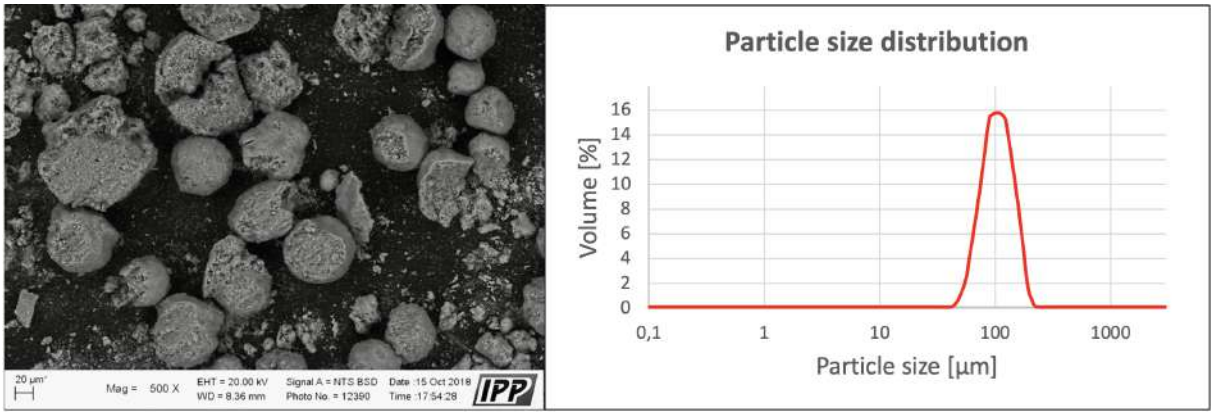

Figure 3.2: Morphology of the HA powder particles (left), and particle size distribution (right) [106]

The purity of the powder stated by the manufacturer was verified by our XRD analysis, confirming 100% HA composition. Of this, 9% were identified as amorphous phase, thus the crystallinity was determined to be 91%.

3.2 RF-ICP deposition

Tekna Tek-15 available at the Institute of Plasma Physics (IPP) in Prague, Czech Academy of Sciences was used as the radio frequency inductively-coupled plasma device for the deposition of HA coatings onto the substrates. The basic working principles of the technology were described in section 2.3. Fig. 3.3 shows the internal arrangement of the device components.

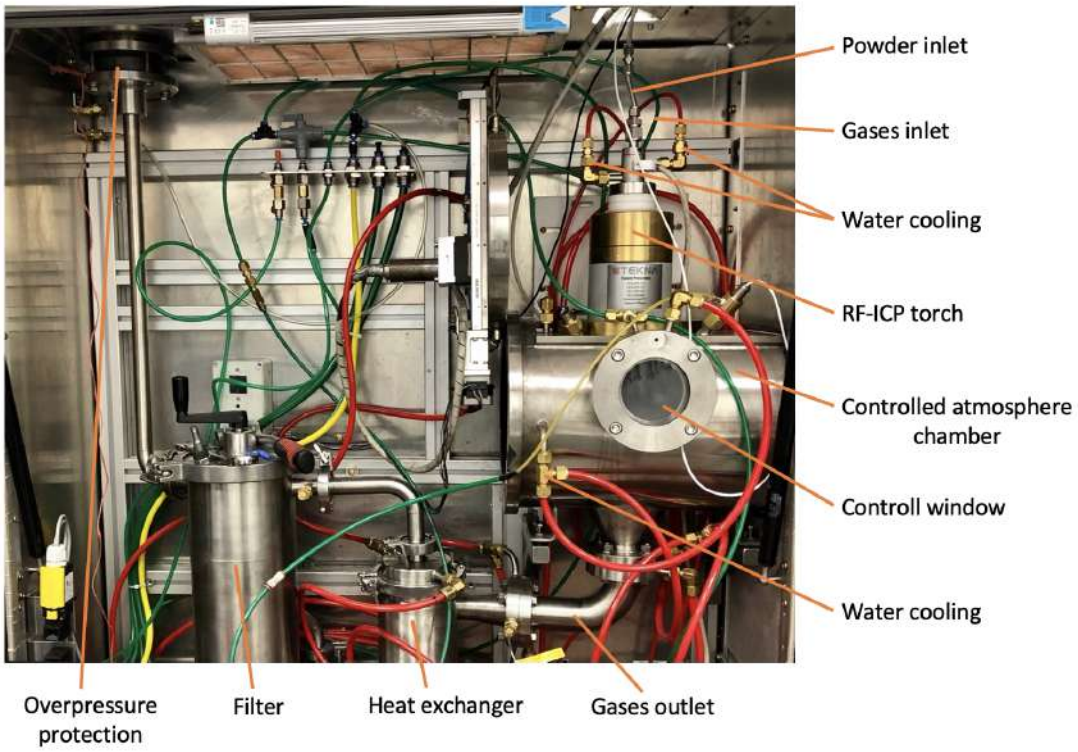

Figure 3.3: Tekna Tek-15 internal arrangement of components

This device could reach up to 15 kW of torch power. The chamber was equipped with an in-house designed and manufactured sample holder that can revolve, move in the axial direction, or combine both. The holder was designed to support up to six substrates simultaneously. Concurrently, the RF-ICP torch placed perpendicular to the holder can move up and down, allowing to set the spraying distance. An external feeder allowing a precise feedrate control was used to transport the HA powder into the torch. All these adjustable parameters were first optimized using the stainless steel substrates, as shown in Table 9. After the optimizations (SR1-SR4), two additional runs were realized using Ti6Al4V substrates (SR5-SR6). The run SR5 copied the successfully optimized parameters (SR4), the run SR6 differed in powder feedrate and spray distance (Table 10).

Table 9: Optimization of RF-ICP spray parameters using AISI 304 substrates

Spraying run	**SR1**	**SR2**	**SR3**	**SR4**
Torch power [kW]	9	12	15	15
Feedrate [g/min]	0.15	0.15	0.15	1.3
Motion	shift	shift	shift	shift + revolution
Spraying distance [mm]	70	70	70	70
Preheat [s]	60	60	60	60
Torch passes	5	5	5	4
Spray time [s]	300	300	300	240

Table 10: RF-ICP deposition on Ti6Al4V substrates

Spraying run	**SR5**	**SR6**
Torch power [kW]	15	15
Feedrate [g/min]	1.3	0.65
Motion	shift + revolution	shift + revolution
Spraying distance [mm]	70	110
Preheat [s]	60	60
Torch passes	4	4
Spray time [s]	240	240

3.3 Coatings analysis

The produced coatings were subjected to several analyzes. First, their surface roughness R_a and R_z was measured using the surface roughness tester Mitutoyo SJ-210. Five measurements along the longer side and five along the shorter one were made to obtain average values.

Phase composition of samples was determined by X-ray diffraction (XRD) method. The measurements were carried out in a symmetrical Bragg-Brentano arrangement on vertical diffractometer Bruker D8 Discover (Bruker AXS, Germany) using Cu Kα radiation with Ni Kβ filter. Diffracted beam was detected by 1D detector LynxEye. The angular range was from 5° to 80° with a step size 0.03°. The total time of each step was 384 s. Phase identification was done using X'Pert HighScore program which accessed PDF-2 database of crystalline phases. Quantitative Rietveld refinement was performed in TOPAS V5 to determine wt.% of all the identified phases.

To asses the coatings' microstructure, the samples were metallographically prepared: they were cut with precise metallographic saw Struers Setocom-50, embedded in Struers EpoFix resin and then hardened for 24 hours. The final samples were polished using automatic polishing system Struers Tegramin-25. Subsequently, they were observed using the backscattered electron mode in Zeiss EVO MA15 scanning electron microscope (SEM).

A set of micrographs (10 images from different parts of the coating for each sample) was further taken by Tescan Vega SEM for porosity determination using the image analysis software ImageJ.

4 Results and discussion

This chapter will present the results of the analyzed HA coatings. The coatings will be evaluated with respect to their microstructure and phase content. The results will be discussed with respect to the selected parameters of the deposition and compared to the available literature sources.

4.1 Surface roughness

The surface roughness plays an essential role in the attachment of the implant to the bone tissue. The tighter a connection of the implant to the bone is, the better transmission of stress without any unfavorable motion between them (abrasion is minimized). Adequate surface roughness is also very important to effectively meet the implant's bioactivity. Bone cells were proven to be very sensitive to micro-topography and they can orient and migrate based on the surface features. It was discovered that a roughness in range of 2.5-4 μm is the best for cell adhesion and growth, while roughness in the range of 4-7 μm makes cell differentiation possible [107][108].

The size of osteoblasts is approximately 20-50 μm, which is also a roughness that they still recognize and grow on. The surface with such roughness appears locally smooth, but the cells can still attach to it and also proliferate [109][110].

Table 11: Surface roughness of applied coatings

	SR4	**SR5**	**SR6**
Ra [μm]	16.00±0.49	17.26±0.83	17.26±1.11
Rz [μm]	79.48±2.57	86.57±3.58	85.32±3.23

Based on the microstructure observation (see section 4.2), only samples SR4-SR6 were recognized as promising. As such, the analyses such as surface roughness were performed using these samples only.

It can be seen that the average roughness of the selected samples (Table 11) lies in the range between the differentiation-promoting micro-roughness and the proliferation-promoting macro-roughness. In other words, from the point of view of satisfactory connection of the implant to the bone tissue, the roughness of the applied coatings is sufficient and meets the stringent conditions.

4.2 Microstructure

Plasma spraying has been used for a long time to apply HA coatings because it is able to ensure sufficient adhesion between the coating and the substrate and, in addition, well-adjustable deposition parameters ensure reproducible results. Besides, it is suitable for mass production. The thickness of HA coatings applied by plasma spray usually ranges from 50-200 μm. However, related to the nature of the process, there are severe drawbacks, such as bioceramic decomposition caused by high temperatures, high thermal residual stresses in the coating, or the presence of defects (unmelted particles, voids or cracks) [28].

To minimize these negative phenomena in the RF-ICP spraying process, the spray parameters were first optimized using AISI 304 substrates. The SEM images of samples SR1-SR4 presented in Fig. 4.1 document this continuous adjustment of the spray parameters.

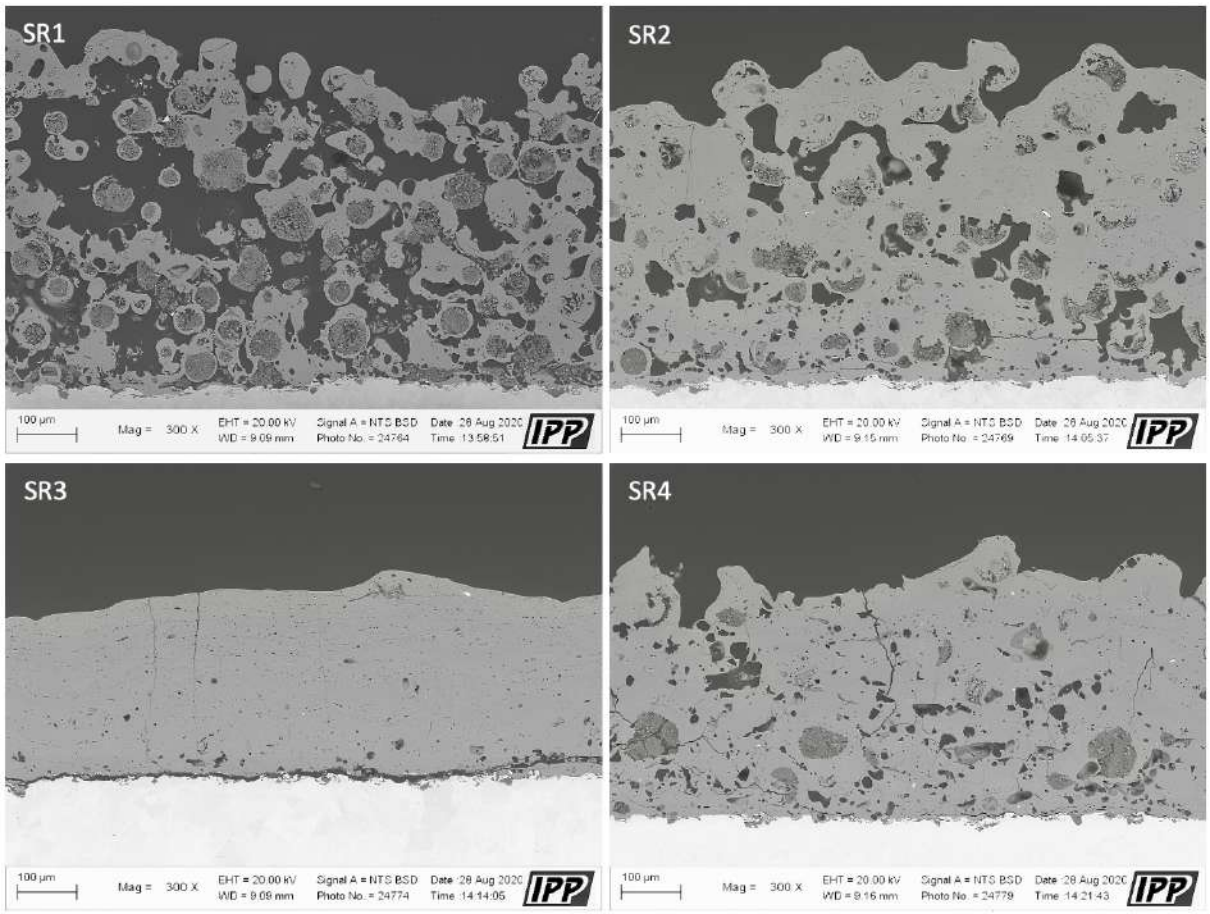

Figure 4.1: Optimization of the process using the AISI 304 substrates

The sample SR1 shows a very porous and discontinuous coating consisting almost entirely of unmelted particles of the HA powder, undoubtedly caused by the low 9 kW power of the plasma torch. Therefore, the power was increased to 12 kW and the spraying was repeated. The obtained sample SR2 shows much less porous coating, more cohesive, but still containing a significant proportion of unmelted particles. To reduce the percentage of unmelted particles, the torch power was further increased to the maximum of the device, 15 kW, and SR3 spraying was carried out. As the SEM image shows, a very dense coating was formed. No unmelted particles were observed in the structure. In fact, the coating was too dense and individual splats could not be discerned. This could have been a consequence of remelting of deposited material caused by the subsequent 15-kW torch passes (five passes were used in total). Despite the mechanical strength such coating would offer, the virtually non-porous coating would be unsuitable for bioapplication. In this regard, it was necessary to adjust other spray parameters. Therefore, for SR4, the substrate motion was modified. All previous coatings were deposited onto substrates that only transversally shifted back and forth relative to the plasma stream. For SR4, the transversal shift was combined with the holder continuous revolution.

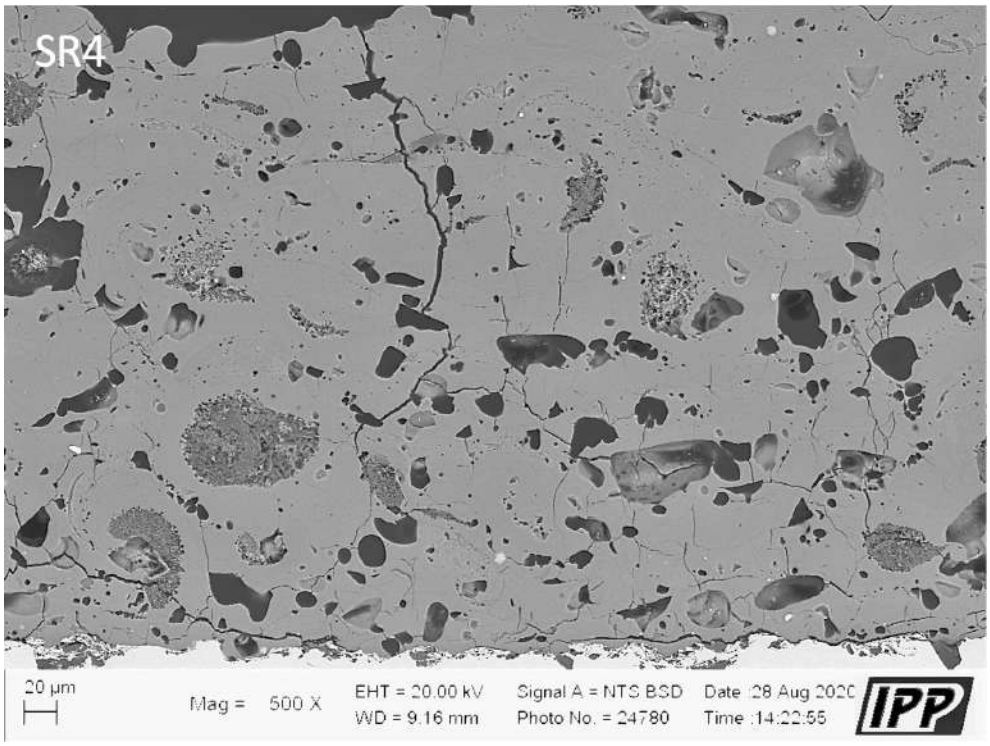

Figure 4.2: SEM image of AISI 304 substrate coated with SR4 parameters

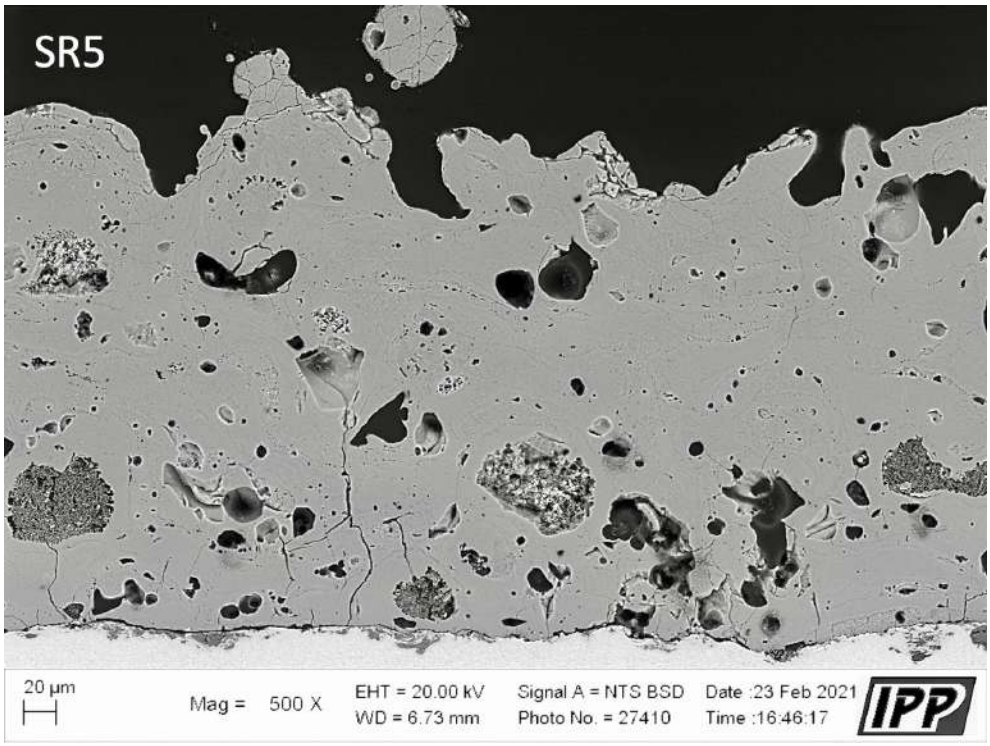

Figure 4.3: SEM image of Ti6Al4V substrate coated with SR5 parameters

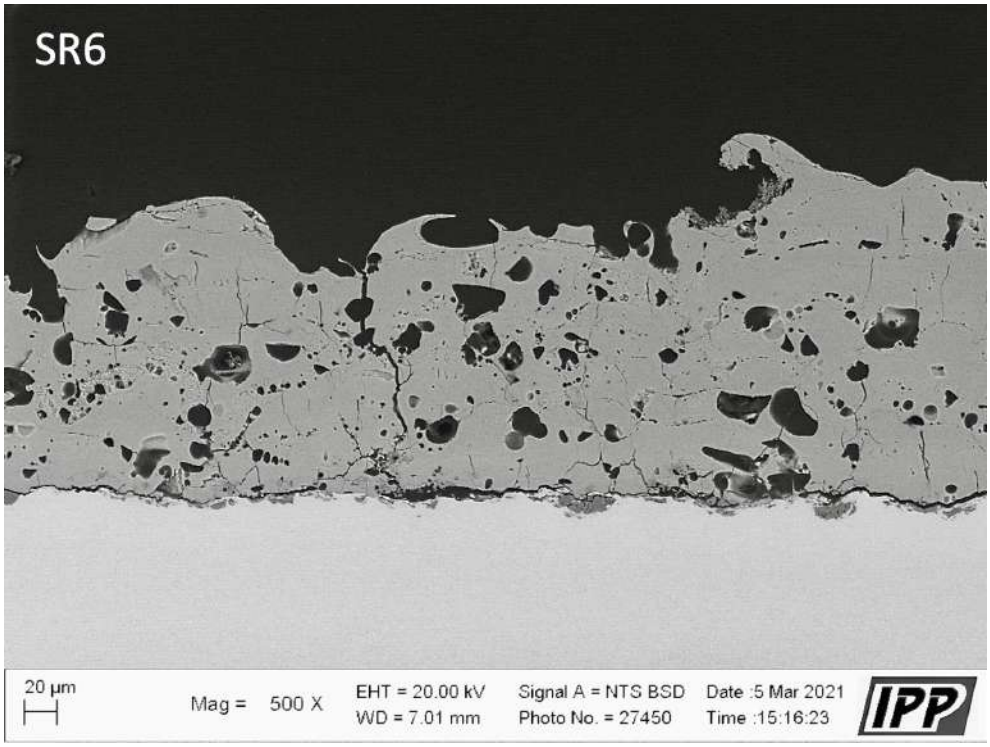

Figure 4.4: SEM image of Ti6Al4V substrate coated with SR6 parameters

This combination of movement allowed to evenly distribute (divide) the 15-kW torch power (by deposition on six substrates), to cool the samples down more effectively (each of the six samples was now sprayed only for a limited time and was cooled intensively when out of the spray-line sight) and also allowed to compensate the Gaussian distribution of the coating thickness that formed in the coatings where reciprocal transversal movement was used only. The resulting coating SR4 was suitably porous, well cohesive and contained an acceptable amount of unmelted, 100% crystalline HA particles. As this microstructure was considered optimal, the substrates were changed to Ti6Al4V and the experiment was further expanded (SR5, SR6).

The SEM images presented in Figs. 4.2, 4.3 and 4.4 show a larger magnification of the sample SR4 compared to samples SR5 and SR6, respectively.

The presented microstructures indicate similarity of the three coatings, with only minor differences. Both samples SR4, SR5 sprayed under identical parameters (except the substrate material) contained vertical cracks, however, the coating on the AISI 304 substrate showed larger cracks at the surface, which the Ti6Al4V substrate seems to have eliminated. This may be caused by different thermal properties of both metals.

To further optimize the properties, another spray parameters were adjusted for SR6 - spray distance and powder feedrate (Table 10). The spray distance was extended so that the deposited HA particles spend longer time in the plasma stream, allowing their better and more uniform melting. At the same time, the powder feedrate was halved to distribute the plasma enthalpy onto less particles, potentially triggering yet more even and stable conditions. Naturally, the lower feedrate would bring a reduction of the coating thickness. However, it was decided not to increase the number of passes under the torch, to prevent overlap of this factor's influence with spray distance and feedrate. The reduced thickness (still suitable for the application) could further prevent a formation of the vertical cracks

observed in SR4 and SR5. As shown in Fig. 4.4, the microstructure of the sample improved slightly (e.g., the absence of unmelted particles), but the vertical cracks were still present in SR6. In other words, this approach did not bring a desired improvement and a further optimization of the microstructure is therefore planned in the following experimental work.

4.3 Porosity

Plasma spraying coatings usually have a porosity in the range of 2-20%. In terms of mechanical properties, the coating with the lowest possible porosity is of course the most desirable, while from the point of view of suitability for osteoblasts, it is necessary to prepare the coating with certain porosity levels. In this respect, a coating with a porosity in the range of 5-20% meets both criteria (retains sufficient mechanical properties and offers good cells compatibility) and therefore is most suitable to use [111][112].

Table 12: Porosity and pore size of selected coatings

	SR4	**SR5**	**SR6**
Porosity [%]	8.58±0.81	8.60±2.07	10.75±1.22
Pore size [μm]	34.27±2.11	29.47±3.75	23.94±1.08

Image analysis (summed up in Table 12) revealed that the substrate type does not play a crucial role in porosity formation: samples SR4 and SR5 were deposited under identical conditions and the porosity of their coatings is more or less the same. In SR6, the powder particles were fed in at a lower feedrate and deposited from a greater deposition distance (spent a longer time in the plasma stream), which could cause more thorough melting of the particles and form less porous coatings. However, coating with a higher porosity has been formed, instead. At the moment, this rather unexpected result needs to be understood yet. At the same time, the average pore sizes were calculated assuming a circular geometry of the pores. The results obtained indicate a decrease in pore size associated with different substrate's thermal properties and deposition parameters.

The porosity levels of the studied samples fall within the range suitable for osteoblast occupancy and may be applicable in terms of biocompatibility with the host tissue. Regarding to ideal pore size, according to Holy et al., the suitable pore size for bone in-growth ranges from 100 μm to 400 μm, while Itala et al. claim the pore size ranges from 50 μm to 125 μm [113][114]. It is therefore noticeable that opinions on the ideal pore size differ in the literature. Nevertheless, it is clear that depending on the size of the osteoblasts (20-50 μm), pores of the same minimum size are needed to allow bone tissue in-growth to occur. The measured values of pore sizes in our coatings, also with regard to the research of Cizek et al., are rather undersized and are not completely suitable for bone tissue in-growth [115]. For this reason, further experiments should be undertaken to achieve larger pore size.

4.4 Phase composition

Plasma spraying of hydroxylapatite coatings has been and still is the most widely used method, since it is still the only method approved by Food and Drug Administration (FDA) for applying coatings onto the implants' surfaces intended for clinical use. Unfortunately, as described earlier in section 2.6.3, HA readily decomposes into undesired phases during plasma deposition, specifically into TCP, TTCP and CaO. In addition to these, dehydroxylated phases such as oxyhydroxylapatite (OHA) and oxyapatite (OA), or quenched phases such as amorphous calcium phosphate (ACP), may also occur [69].

Of the potential options, the most widespread plasma spray technology is undoubtedly atmospheric plasma spray (APS). This technology is well researched, tested for years and its results are very good. However, even this technology has room for improvement, thus other techniques for applying HA coatings are being explored. These researches have focused, for example, on processes such as low-pressure (vacuum) plasma spraying (LPPS/VPS [116]), suspension plasma spraying (SPS [117]), solution precursor plasma spraying (SPPS [118]), microplasma spraying (MIPS [119]) and low-energy plasma spraying (LEPS [120]). This serie was now supplemented with RF-ICP technology used for our HA deposition from this study. The phase composition of the RF-ICP HA coatings SR4-SR6 is presented in Figs. 4.5-4.7.

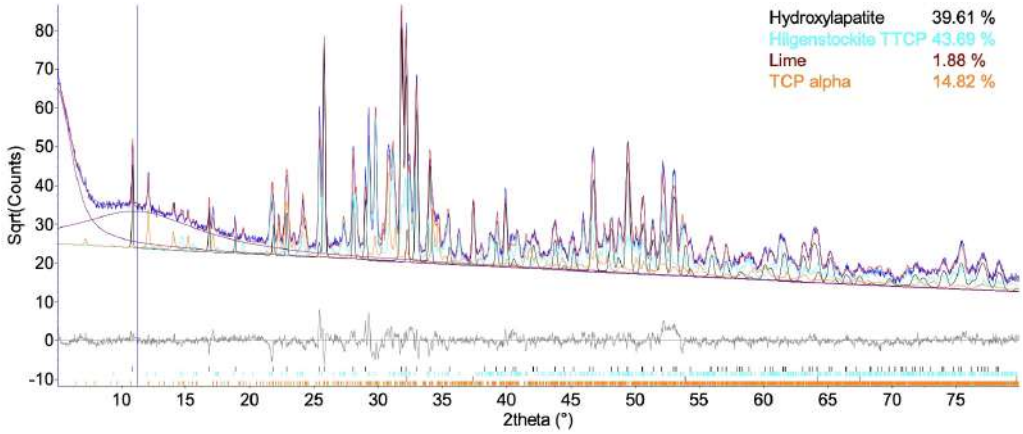

Figure 4.5: XRD pattern of sample SR4

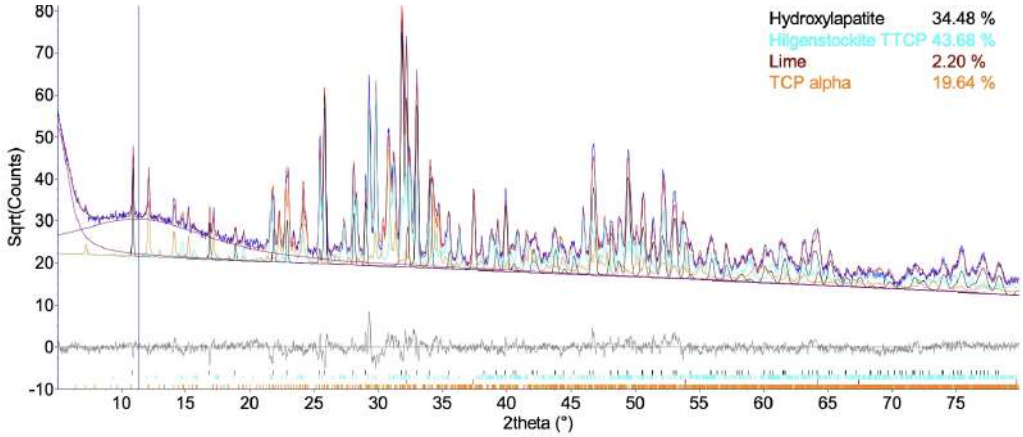

Figure 4.6: XRD pattern of sample SR5

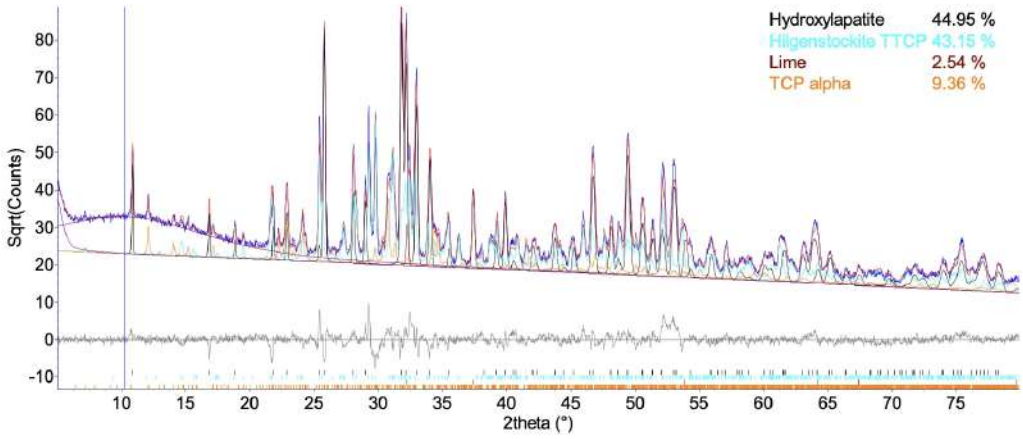

Figure 4.7: XRD pattern of sample SR6

Quantification of the phase content by Rietveld analysis is summarized in Table 13. Despite the lowest content of unmolten particles, of the original, 100% HA powder, the sample SR6 exhibited the highest content of HA. The differences may be triggered by the different thermal conditions during the deposition of the three samples. The TTCP phase accounted for more than 40% of all coatings, α-TCP about 10-20%, and CaO was present in small amounts.

Table 13: XRD analysis of selected samples (all in wt.%)

	SR4	**SR5**	**SR6**
HA	39.6	34.5	45.0
TTCP	43.7	43.7	43.2
α-TCP	14.8	19.6	9.4
CaO	1.9	2.2	2.5

In the literature, coatings applied by conventional atmospheric plasma spray with HA content as high as 90% with a low content of decomposed α-TCP and TTCP phases can be found [121]. Also in the case of suspension plasma spray, coatings containing almost 80% of HA and small amounts of α-TCP, TTCP and CaO were achieved [122].

In comparison, the trial RF-ICP coatings presented herein have a significantly lower HA content and a relatively high content of undesired phases. In this respect, further process optimization is needed to achieve the quality of DC plasma sprayed coatings researched for decades.

5 Conclusions

The aim of the present diploma thesis was to explore a new possibility of applying bioactive coatings on metal substrates with a possible overlap into clinical use. Conventional and commonly available alloys used in bioapplications, specifically stainless steel AISI 304 and titanium alloy Ti6Al4V, were chosen as substrates. Hydroxylapatite powder was chosen as the coating material, which is used mainly for orthopedic and dental applications due to its excellent bioactive properties. The unexplored novelty of this research has been the use of radio frequency inductively-coupled plasma (RF-ICP) technology as an energy source for the ceramic coatings deposition.

The stainless steel substrates were use to optimize the deposition process. Once the optimum conditions were identified, deposition was performed on the titanium alloy substrates. The produced coatings were subjected to analyzes in terms of surface roughness, microstructure (porosity and pore size) and phase composition (X-ray diffraction).

The surface roughness of all samples was found to be satisfactory in terms of potential sufficient adhesion of osteoblasts, providing favorable conditions for new bone growth. In terms of microstructure, SEM imaging confirmed the splat structure typical for plasma sprayed coatings. The trial coatings contained a significant proportion of unmelted particles, that were succesfully eliminated to a satisfactory level in subsequent optimization. Contrary to this, the occurrence of vertical cracks was not eliminated in this study and remains an issue to be further resolved in the next experiments. The overall porosity content of the coatings was satisfactory from a biological and mechanical point of view in all directions. However, the pore size for bone in-growth was shown to be still slightly insufficient. Finally, the XRD analysis revealed that the low powers of the RF-ICP torch as opposed to the high-power atmospheric DC sources did not trigger favorable phase content. In fact, the RF-ICP coatings' phase composition change more prominently and the 100% pure hydroxylapatite feedstock powder decomposed into various phases during its deposition. The HA content in the coatings ranged from 35-45%. Compared to the best results obtained by the conventional atmospheric plasma spray deposition or suspension plasma spray deposition, these are about half the values. Further optimization will be pursued in the planned experiments.

In summary, the RF-ICP technology shows a promising potential for deposition of HA coatings. At the same time, there is still a need for improvement as the obtained coatings do not reach the quality of the best results obtained in the literature when spraying using atmospheric torches. In particular, the phase composition need to be controlled to partially suppress the formation of secondary phases. Further experimental work is planned to target these issues.

6 Bibliography

[1] XU, B.; ZHANG, W.: Progress and application of nano-surface engineering in China. Oxford: Elsevier Science, 2005, 339-343. ISBN 978-0-08-044504-5. URL: https://-doi.org/10.1016/B978-008044504-5/50070-2

[2] QUINTINO, L.: 1 - Overview of coating technologies. Woodhead Publishing, 2014, 1-24. ISBN 978-0-85709-468-1. URL: https://doi.org/10.1533/9780857094698.1

[3] What are the main surface engineering processes? TWI [online]. Cambridge: TWI, 2021 [2021-02-22]. URL: https://bit.ly/3eAyPdh

[4] HUTCHINGS, I.; SHIPWAY, P.: 7 - Surface engineering. Butterworth-Heinemann, 2017, s. 237-281. ISBN 978-0-08-100910-9. URL: https://doi.org/10.1016/B978-0-08-100910-9.00007-6

[5] An Introduction to Thermal Spray. In: Sulzer Metco [online]. Germany: Sulzer Metco, 2013 [2021-02-24]. URL: https://bit.ly/3kXNzns

[6] HUMÁR, A.: Materiály pro řezné nástroje: Interaktivní multimediální text pro všechny studijní programy FSI [online]. In: Brno: VUT FSI, 2006 [2021-5-3]. URL: https://bit.ly/2SixwGt

[7] BUNSHAH, R.: Handbook of hard coatings: deposition technologies, properties and applications. 2001/01/01. ISBN 0815514387.

[8] KŘÍŽ, A.: Tenké vrstvy [online]. Plzeň, 2005 [2021-5-3]. Presentation. Západočeská univerzita v Plzni. URL: https://bit.ly/3nKTwFW

[9] MARTIN, P. M.: Chapter 6 - Ion Plating. Handbook of Deposition Technologies for Films and Coatings. 3rd edition. Boston: William Andrew Publishing, 2010, 297-313. ISBN 978-0-8155-2031-3. URL: https://doi.org/10.1016/B978-0-8155-2031-3.00006-5

[10] What is electroplating? SPC [online]. 2021 [2021-5-3]. URL: https://bit.ly/3tT9S0l

[11] History. Knowledge Podium [online]. India: Knowledge Podium & BEN, 2020 [2020-11-06]. URL: https://bit.ly/3rJ7tW5

[12] The History of Thermal Spray in a Nutshell. A&A Coatings [online]. South Plainfield, NJ [2020-11-06]. URL: https://bit.ly/2MZ7Egy

[13] PATIÑO-INFANTE, M.; MARINO, A.: Iron based coatings deposited by arc thermal spray. Revista Facultad de Ingenieria. 2017/06/01, 2017, 31-35. DOI: 10.17533/udea.redin.n83a04

[14] POURMOUSA ABKENAR, A.: Wire-arc spraying system: Particle production, transport, and deposition. Toronto, 2007. Doctoral dissertation. University of Toronto.

[15] DUKOVSKÝ, D.: Charakterizace nástřiků deponovaných suspenzním plasmovým nanášením s použitím různých organických nosičů. Brno, 2019. Bakalářská práce. Vysoké učení technické v Brně. Vedoucí práce Jan Čížek.

[16] TUCKER, R. C.: Thermal Spray Coatings. COTTEL, C. M.; SPRAGUE, J. A.; SMIDT, F. A.: ASM Handbook Volume 5: Surface Engineering [online]. 5th edition. Materials Park, OH: ASM International, 1994, 497-509 [2020-11-06]. ISBN 978-0-87170-384-2. URL: https://bit.ly/30qbgv4

[17] Žárové stříkání. In: PLASMAMETAL [online]. Brno: PLASMAMETAL , 2021 [2021-03-01]. URL: https://www.plasmametal.cz/zarove-strikani

[18] VARDELLE, A.; MOREAU, C.; AKEDO, J.; et al.: The 2016 Thermal Spray Roadmap. Journal of Thermal Spray Technology. 2016/12/01, 25. DOI: 10.1007/s11666-016-0473-x

[19] MUŠÁLEK, R.: Inženýrské výzvy v oblasti žárového stříkání [online]. Presentation. [2021-04-16]. URL: https://bit.ly/3v7WmIe

[20] AMIN, S.: A Review on Thermal Spray Coating Processes. International Journal of Current Trends in Engineering & Research (IJCTER) [online]. 2016(4), 556-563 [2021-03-09]. ISSN 2455–1392. URL: https://bit.ly/3qExXqp

[21] DAVIS, J. R.: Handbook of Thermal Spray Technology. ASM International, 2004. ISBN 08-717-0795-0.

[22] PUDDU, P.; POPA, S.; BOLELLI, G.; et al.: Suspension HVOF spraying of TiO_2 using a liquid-fueled torch [on-line]. 2018, 349, 677-694 [2021-05-06]. ISSN 0257-8972. URL: https://bit.ly/38qrAk1

[23] Thermal spray systems. Flame spray technologies [online]. Netherlands: Flame Spray Technologies B.V., 2021 [2021-03-08]. URL: https://bit.ly/2Oj3jph

[24] Arc Wire Thermal Spray Process. Thermal Spray Coatings - Gordon England [online]. Farnham: Gordon England, 1996-2018 [2021-05-06]. URL: https://www.gordonengland.co.uk/aws.htm

[25] Plasma. In: UCAR Center for science education [online]. Boulder: UCAR, 2021 [2021-03-10]. URL: https://scied.ucar.edu/learning-zone/sun-space-weather/plasma

[26] CHABERT, P.; BRAITHWAITE, N.: Physics of Radio-Frequency Plasmas [online]. Cambridge: Cambridge University Press, 2011 [2021-03-10]. ISBN 9780511974342. DOI: 10.1017/CBO9780511974342

[27] VARDELLE, A.; MOREAU, C.; THEMELIS, N.; et al.: A Perspective on Plasma Spray Technology. Plasma Chemistry and Plasma Processing. 2014/12/11, 35. DOI: 10.1007/s11090-014-9600-y

[28] WANG, M.: 6 - Composite coatings for implants and tissue engineering scaffolds. Woodhead Publishing Series in Biomaterials. Woodhead Publishing, 2010, 127-177. ISBN 978-1-84569-436-4. URL: https://bit.ly/3qvkkcT

[29] FAUCHAIS, P. L.: Thermal spray fundamentals: from powder to part. New York, NY: Springer Science+Business Media, LLC, 2013. ISBN 978-0-387-28319-7.

[30] What types of plasma spraying equipment are available? In: TWI Ltd. [online]. Cambridge: TWI, 2021 [2021-03-09]. URL: https://bit.ly/3ccHC2c

[31] OKUMURA, T.: Inductively Coupled Plasma Sources and Applications. Physics Research International. 2010/02/20. DOI: 10.1155/2010/164249

[32] GUO, Q.; ZHAO, P.; LI, L.; et al.: The effect of hydrogen on B_4C coatings fabrication in inductively coupled plasma torch. AIP Advances. 2018/02/01, 8, 025003. DOI: 10.1063/1.5011782

[33] HERMAN, V.: Stanovení mikro a makro prvků v balených vodách technikou ICP-OES. Brno, 2015. Master's thesis. Brno university of technology.

[34] NEIKOV, O. D.; YEFIMOV, N. A.: Chapter 1 - Powder Characterization and Testing. Oxford: Elsevier, 2019, 3-62. ISBN 978-0-08-100543-9. URL: https://-doi.org/10.1016/B978-0-08-100543-9.00001-4

[35] NEALE, Z.: Inductively coupled plasma optical emission spectroscopy (ICP-OES) Overview. Youtube [online]. 24.4.2020 [2021-05-03]. URL: https://bit.ly/3eZhkCQ

[36] ICP-MS. Radboud University [online]. Netherlands: Radboud University, 2021 [2021-03-13]. URL: https://bit.ly/38SzJOD

[37] MIHALJEVIČ, M.; STRNAD, L.; ŠEBEK, O.: Využití hmotnostní spektrometrie s indukčně vázaným plazmatem v geochemii. Chemické listy [online]. 2004, (98), 123-130 [2021-03-13]. ISSN 1213-7103. URL: https://bit.ly/3tX4Dgl

[38] MESTEK, O.: Hmotnostní spektrometrie s indukčně vázaným plazmatem: pracovní text pro Podzemní výukové středisko JOSEF [online]. Praha: Vysoká škola chemicko-technologická v Praze, 2010 [2021-03-13]. URL: https://bit.ly/3t9r3Lc

[39] What is Single Particle ICP-MS? Tofwerk [online]. Thun, Switzerland: Tofwerk, 2021 [2021-05-03]. URL: https://www.tofwerk.com/single-particle-icp-ms/

[40] SOLANKI, A.; UM, H.: Chapter Two - Top-Down Etching of Si Nanowires. Nanowires for Energy Applications. 98. Elsevier, 2018, 71-149. ISSN 0080-8784. URL: https://doi.org/10.1016/bs.semsem.2018.04.001

[41] LISHAN, D. G.: Plasma Etching: Comparing PE, RIE and ICP-RIE. Plasma-Therm [online]. St. Petersburg: Plasma-therm, 2020 [2021-04-06]. URL: https://bit.ly/3wwJKuP

[42] HENRY, M. D.: ICP etching of silicon for micro and nanoscale devices. California, 2010. Thesis. California Institute of Technology.

[43] ZHENG, Y.; YE, H.; LIU, J.; et al.: Surface morphology evolution of a polycrystalline diamond by inductively coupled plasma reactive ion etching (ICP-RIE). Materials Letters. 2019, 253, 276-280. ISSN 0167-577X. URL: https://doi.org/10.1016/j.mat-let.2019.06.079

[44] CONNORS, M. K.; PLANT, J.; RAY, K.; et al: Chamber conditioning process development for improved inductively coupled plasma reactive ion etching of GaAs/AlGaAs materials. Journal of Vacuum Science Technology B: Microelectronics and Nanometer Structures. 2013/03/01, 31, 1207. DOI: 10.1116/1.4792839

[45] XU, J. L.; KHOR, K. A.; GU, Y. W.; et al.: Radio frequency (rf) plasma spheroidized HA powders: powder characterization and spark plasma sintering behavior. Biomaterials. 2005, 26(15), 2197-2207. ISSN 0142-9612. URL: https://bit.ly/2NEEgMZ

[46] QIN, Q.; YANG, F.; SHI, T.; et al.: Spheroidization of tantalum powder by radio frequency inductively coupled plasma processing. Advanced Powder Technology. 2019, 30(8), 1709-1714. ISSN 0921-8831. URL: https://doi.org/10.1016/j.apt.2019.05.022

[47] NAM, J.-S.; PARK, E.; SEO, J.-H.: Numerical Analysis of Radio-Frequency Inductively Coupled Plasma Spheroidization of Titanium Metal Powder Under Single Particle and Dense Loading Conditions. Metals and Materials International. 2019/07/11, 26. DOI: 10.1007/s12540-019-00348-6

[48] HUR, M.; LEE, D.; YANG, S.; et al.: Numerical Modeling of Nano-powder Synthesis in a Radio-Frequency Inductively Coupled Plasma Torch. Applied Science and Convergence Technology. 2018/01/31, 27, 14-18. DOI: 10.5757/ASCT.2018.27.1.14

[49] DOROZHKIN, S. V.: Calcium orthophosphate bioceramics. Ceramics International. 2015, 41(10, Part B), 13913-13966. ISSN 0272-8842. URL: https://-doi.org/10.1016/j.ceramint.2015.08.004

[50] PARIDA, P.; BEHERA, A.; MISHRA, S. C.: Classification of Biomaterials used in Medicine. International Journal of Advances in Applied Sciences (IJAAS) [online]. 2012, 1(3), 31-35 [2021-04-07]. ISSN 2252-8814. URL: https://bit.ly/3fyd10K

[51] PARK, J. B.; LAKES, R. S.: Biomaterials: An Introduction. 3rd Ed. New York: Springer, 2007. ISBN 978-0-387-37880-0.

[52] ŠIMŮNEK, A.: Dentální implantologie. 2. vydání. Hradec Králové: Nucleus HK, 2008, 285. ISBN 978-808-7009-307

[53] KAUR, M.; SINGH, K.: Review on titanium and titanium based alloys as biomaterials for orthopaedic applications. Materials Science and Engineering: C. 2019, 102, 844-862. ISSN 0928-4931. URL: https://doi.org/10.1016/j.msec.2019.04.064

[54] DUCHEYNE, P.; HASTINGS, G.: Metal and ceramic biomaterials: Volume II strength and surface. 2018/01/18, 172, 1. ISBN 9781351074438. DOI: 10.1201/9781351074438

[55] BROVOLD, M.; ALMEIDA, J.; PLA, I.; et al.: Naturally-Derived Biomaterials for Tissue Engineering Applications. Novel Biomaterials for Regenerative Medicine. 1077. 2018/01/01, 421-449. ISBN 978-981-13-0946-5. DOI: 10.1007/978-981-13-0947-2_23

[56] RAUT, H.; DAS, R.; LIU, Z.; et. al.: Biocompatibility of Biomaterials for Tissue Regeneration or Replacement. Biotechnology Journal. 2020/07/12, 15, 2000160. DOI: 10.1002/biot.202000160

[57] MORRISON, E.; SUVARNAPATHAKI, S.; BLAKE, L.; et al.: Unconventional biomaterials for cardiovascular tissue engineering. Current Opinion in Biomedical Engineering. 2021, 17, 100263. ISSN 2468-4511. URL: https://-doi.org/10.1016/j.cobme.2021.100263

[58] ISHIKAWA, K.; MATSUYA, S.; MIYAMOTO, Y.; et al.: 9.05 - Bioceramics. Oxford: Pergamon, 2003, 169-214. ISBN 978-0-08-043749-1. URL: https://-doi.org/10.1016/B0-08-043749-4/09146-1

[59] PRECNEROVÁ, M.; BODIŠOVÁ, K.; FRAJKOROVÁ, F.; et al.: In vitro bioactivity of silicon nitride–hydroxyapatite composites. Ceramics International. 2015, 41(6), 8100-8108. ISSN 0272-8842. URL: https://doi.org/10.1016/j.ceramint.2015.03.011

[60] HANAWA, T.: Metal ion release from metal implants. Materials Science and Engineering: 2004, 24(6), 745-752. ISSN 0928-4931. URL: https://-doi.org/10.1016/j.msec.2004.08.018

[61] HARUN, W.; ASRI, R.; ALIAS, J.; et al.: A comprehensive review of hydroxyapatite-based coatings adhesion on metallic biomaterials. Ceramics International. 2018, 44(2), 1250-1268. ISSN 0272-8842. URL: https://doi.org/10.1016/j.ceramint.2017.10.162

[62] KURTZ, S.; ONG, K.; LAU, E.; et al.: Projections of Primary and Revision Hip and Knee Arthroplasty in the United States from 2005 to 2030. The Journal of bone and joint surgery. American volume. 2007/04/01, 89, 780-5. DOI: 10.2106/JBJS.F.00222

[63] RATNER, B.: Biomaterials Science, Second Edition: An Introduction to Materials in Medicine. XII. 2003/12/01. DOI: 10.1016/B978-0-08-050014-0.50004-3

[64] PARK, J.; LAKES, R.S.: Biomaterials: An introduction: Third edition. Springer. NY, 2007/01/01, 1-561.

[65] DAVIS, J. R.: Handbook of Materials for Medical Devices. Metallic materials. 2003/01/01.

[66] PLANELL, J. A.; BEST, S.; LACROIX, D.; et al.: Bone repair biomaterials. Cambridge: Woodhead publishing, 2009/08/01, 496. ISBN 9781845693855.

[67] MCANDREW, A.: Modelling of Ti-6Al-4V Linear Friction Welds. Cranfield, 2015. Dissertation. Cranfield University.

[68] D is for Duplex Titanium Alloys, Part 2. MetalsAndAlloysBlog [online]. MetalsAndAlloysBlog, 2021, 20.11.2016 [2021-5-4]. URL: https://bit.ly/3eVtL2A

[69] HEIMANN, R. B.: Plasma-Sprayed Hydroxylapatite Coatings as Biocompatible Intermediaries Between Inorganic Implant Surfaces and Living Tissue. Journal of Thermal Spray Technology. 2018, 27(8), 1212-1237. ISSN 1544-1016. DOI: 10.1007/s11666-018-0737-8

[70] BEST, S. M.; PORTER, A. E.; THIAN, E. S.; et al.: Bioceramics: Past, present and for the future. Journal of the European Ceramic Society. 2008, 28(7), 1319-1327. ISSN 0955-2219. URL: https://doi.org/10.1016/j.jeurceramsoc.2007.12.001

[71] URBAN, Z; STRNAD, Z.: Bioaktivní sklokeramika nahrazující kost: Neživé náhrady srůstající s živou tkání. Vesmír [online]. Vesmír, 2000, 79(130) [2021-04-16]. ISSN 1214-4029. URL: https://bit.ly/3stNtWF

[72] Biokeramika a biomimetické procesy. In: Vysoká škola chemicko-technologická v Praze [online]. Praha. 2021 [2021-04-16]. URL: https://bit.ly/3e9Hmlf

[73] PRECNEROVÁ, M.; BODIŠOVÁ, K.; FRAJKOROVÁ, F.; et al.: In vitro bioactivity of silicon nitride–hydroxyapatite composites. Ceramics International. 2015, 41(6), 8100-8108. ISSN 0272-8842. URL: https://doi.org/10.1016/j.ceramint.2015.03.011

[74] SCHRÖDTER, K.; BETTERMANN, G.; STAFFEL, T.; et al.: Phosphoric Acid and Phosphates. 2008/01/15. ISBN 9783527306732. DOI: 10.1002/14356007.a19_465.pub3

[75] JEONG, J.; KIM, J. H.; SHIM, J. H.; et al.: Bioactive calcium phosphate materials and applications in bone regeneration. Biomaterials Research. 2019, 23(1), 4. ISSN 2055-7124. DOI: 10.1186/s40824-018-0149-3

[76] CIFTCIOGLU, R.: The Preparation and Characterization of Hydroxyapatite Bioceramic Implant Material. Izmir, Turkey, 2000. Disertation. Izmir Institute of Technology.

[77] HENESS, G.; BEN-NISSAN, B.: Innovative Bioceramics. Materials Forum. 2003/11/30, 27, 104-114. URL: https://bit.ly/3tyZwUg

[78] PALOU, M.; KUZIELOVÁ, E.: Biokompatibilné anorganické materiály pre medicínské aplikácie. In.: ONDREJKOVIČOVÁ, I.; HOJEROVÁ, J.; HUDECOVÁ, D.; et al.: Spoločná budúcnosť chémie a biológie [online]. Slovensko: Slovenská technická univerzita v Bratislave, 2006, 69-77 [2021-04-20]. ISBN 80-227-2456-4. URL: https://bit.ly/3gmnf6g

[79] BOIVIN, G.: The hydroxyapatite crystal: A closer look. Medicographia. 2007/01/01, 29, 126-132. URL: https://bit.ly/32vsMPL

[80] Hing, K. A.: Bone repair in the twenty-first century: biology, chemistry or engineering? Philosophical Transactions of the Royal Society of London Series a Mathematical, Physical and Engineering Sciences, 2004. 362(1825): 2821-2850

[81] NAKANO, T.; KAIBARA, K.; TABATA, Y.; et al.: Unique alignment and texture of biological apatite crystallites in typical calcified tissues analyzed by microbeam X-Ray diffractometer system. Bone. 2002/11/01, 31, 479-87. DOI: 10.1016/S8756-3282(02)00850-5

[82] BEZNOSKOVÁ SEYDLOVÁ, M.: Biologické vlastnosti titanové slitiny povlečené hydroxyapatitem ve vztahu k přímému zatížení dentálního implantátu. Praha, 2006. Dissertation. First Faculty of Medicine, Charles University.

[83] BERMAN, A. T.; SPENCE, J. R.; YANICKO, D. R.; et al.: Thermally Induced Bone Necrosis in Rabbits: Relation to Implant Failure in Humans: Relation to Implant Failure in Humans. Clinical Orthopaedics and Related Research. 1984, PMID 6723155. URL: https://bit.ly/3dztS3u

[84] COX, S.: Synthesis methods of hydroxyapatite. Ceram [online]. Staffordshire, UK: Ceram, 2014 [2021-5-2]. URL: https://bit.ly/3xFRTh0

[85] COX, S.; WALTON, R.; MALLICK, K.: Comparison of techniques for the synthesis of hydroxyapatite. Bioinspired, Biomimetic and Nanobiomaterials. 2014/06/01, 4, 37-47. DOI: 10.1680/bbn.14.00010

[86] NUNES, D.; PIMENTEL, A.; SANTOS, L.; et al.: 2 - Synthesis, design, and morphology of metal oxide nanostructures. Metal Oxides. Elsevier, 2019, s. 21-57. ISBN 978-0-12-811512-1. URL: https://doi.org/10.1016/B978-0-12-811512-1.00002-3

[87] PRAMANIK, S.; AGARWAL, A.; RAI, K. N.; et al.: Development of High Strength Hydroxyapatite by Solid-State-Sintering Process. Ceramics International. 2007/04/01, 419-426. DOI: 10.1016/j.ceramint.2005.10.025

[88] PADMANABHAN, S. K.; BALAKRISHNAN, A.; CHU, M.-C.; et al.: Sol–gel synthesis and characterization of hydroxyapatite nanorods. Particuology. 2009, 7(6), 466-470. ISSN 1674-2001. URL: https://doi.org/10.1016/j.partic.2009.06.008

[89] TAS, A. C.: Combustion Synthesis of Calcium Phosphate Bioceramic Powders. Journal of the European Ceramic Society. 2000/12/01, 20, 2389-2394. DOI: doi:10.1016/S0955-2219(00)00129-1

[90] LIM, G.-K.; NG, S.-C.; GAN, L. M.: Processing of Hydroxyapatite via Microemulsion and Emulsion Routes. Biomaterials. 1997/11/01, 18, 1433-9. DOI: 10.1016/S0142-9612(97)00081-1

[91] SUN, L.; BERNDT, C. C.; GREY, C. P.: Phase, structural and microstructural investigations of plasma sprayed hydroxyapatite coatings. Materials Science and Engineering: A. 2003, 360(1), 70-84. ISSN 0921-5093. URL: https://-doi.org/10.1016/S0921-5093(03)00439-8

[92] Superior Hydroxyapatite Coatings for Medical Implants. In: Himed [online]. NY: Himed, 2021 [2021-04-17]. URL: https://www.himed.com/hydroxyapatite-coatings

[93] QIANG, W.; JIN, Z.; LIJUN, Z.; et al.: Investigation and Application of HA Composite Coating on the Ti Alloy. 2013/05/14, 361-436. ISBN 9780429111389. DOI: 10.1201/b14803-8

[94] KIM, H.; CAMATA, R.; VOHRA, Y; et al.: Control of phase composition in hydroxyapatite/tetracalcium phosphate biphasic thin coatings for biomedical applications. Journal of materials science. Materials in medicine. 2005/11/01, 16, 961-966. DOI: 10.1007/s10856-005-4430-3

[95] KLEIN, C.; BLIECK-HOGERVORST, J. M.; WOLKE, J.; et al.: Studies of the Solubility of Different Calcium-Phosphate Ceramic Particles In Vitro. Biomaterials. 1990/10/01, 11, 509-12. DOI: 10.1016/0142-9612(90)90067-Z

[96] KIM, H.; VOHRA, Y.; LOUIS, P.; et al.: Biphasic and Preferentially Oriented Microcrystalline Calcium Phosphate Coatings: In Vitro and In Vivo Studies. Key Engineering Materials. 2005/04/15, 284-286, 207-210. URL: www.scientific.net/KEM.284-286.207

[97] HEUGHEBAERT, M.; LEGEROS, R.; GINESTE, M.; et al.: Physico-Chemical Characterization of Deposits Associated With HA Ceramics Implanted in Nonosseous Sites. Journal of biomedical materials research. 1988/12/01, 22, 257-68. DOI: 10.1002/jbm.820221406

[98] WENG, J.; LIU, X.-G.; LI, X.-D.; et al.: Intrinsic factors of apatite influencing its amorphization during plasma-spray coating. Biomaterials. 1995, 16(1), 39-44. ISSN 0142-9612. URL: https://doi.org/10.1016/0142-9612(95)91094-F

[99] CARRODEGUAS, R.; AZA, S.: A-Tricalcium Phosphate: Synthesis, Properties and Biomedical Applications. Acta biomaterialia. 2011/06/25, 7, 3536-46. DOI: 10.1016/j.actbio.2011.06.019

[100] MOSEKE, C.; GBURECK, U.: Tetracalcium phosphate: Synthesis, properties and biomedical applications. Acta Biomaterialia. 2010, 6(10), 3815-3823. ISSN 1742-7061. URL: https://doi.org/10.1016/j.actbio.2010.04.020

[101] MONMA, H.; GOTO, M.; NAKAJIMA, H.; et al.: Preparation of tetracalcium phosphate. Gypsum Lime, 1986, 202: 151-5.

[102] MOHAMMADI, Z.; ZIAEI-MOAYYED, A.; SHEIKH, A.; et al.: Analytically Modeling of In Vitro Calcium Dissolution of Plasma-Sprayed Hydroxyapatite Coatings. Iranian Journal of Pharmaceutical Sciences. Materials Science and Engineering Department, Sharif University of Technology, Tehran, Iran, 2008, 4(3), 209-216. ISSN 1735-2444. URL: http://www.ijps.ir/article_2038.html

[103] SOBCZAK-KUPIEC, A.; WZOREK, Z.: The influence of calcination parameters on free calcium oxide content in natural hydroxyapatite. Ceramics International. 2012, 38(1), 641-647. ISSN 0272-8842. URL: https://doi.org/10.1016/j.ceramint.2011.06.065

[104] Chemické složení korozivzdorných ocelí. Italinox [online]. Czech: Italinox, 2021 [2021-04-20]. URL: https://bit.ly/2QHuyuB

[105] Titan Grade 5 (6Al-4V). Bibus Metals [online]. Brno: Bibus Metals, 2021 [2021-04-20]. URL: https://bit.ly/2QiBnmn

[106] MEDICOAT. Certificate of conformity: Hydroxyapatite. France, 2013.

[107] DALBY, M.; GADEGAARD, N.; OREFFO, R.: Harnessing nanotopography and integrin-matrix interactions to influence stem cell fate. Nature materials. 2014/05/21, 13, 558-69. DOI: 10.1038/nmat3980

[108] STOUT, D.; YOO, J.; SANTIAGO, A.; et al.: Mechanisms of greater cardiomyocyte functions on conductive nanoengineered composites for cardiovascular application. International journal of nanomedicine. 2012/11/13, 7, 5653-69. DOI: 10.2147/IJN.S34574

[109] ELLINGSEN, J.: Surface configurations of dental implants. Periodontology 2000. 1998/07/01, 17, 36-46. DOI: 10.1111/j.1600-0757.1998.tb00121.x

[110] QIU, Z.-Y.; CUI, Y.; WANG, X.-M.: Chapter 1 - Natural Bone Tissue and Its Biomimetic. Woodhead Publishing Series in Biomaterials. Woodhead Publishing, 2019, 1-22. ISBN 978-0-08-102717-2. URL: https://doi.org/10.1016/B978-0-08-102717-2.00001-1

[111] FAUCHAIS, P.: Understanding plasma spraying. J Phys D Appl Phys 37(9):R86-R108. Journal of Physics D Applied Physics. 2004/05/01, 37, 86. DOI: 10.1088/0022-3727/37/9/R02

[112] GROSS, K; WALSH, W; SWARTS, E.: Analysis of Retrieved Hydroxyapatite-Coated Hip Prostheses. Journal of Thermal Spray Technology. 2004/06/01, 13, 190-199. DOI: 10.1361/10599630418112

[113] HOLY, C. E.; FIALKOV, J. A.; DAVIES, J.; et al.: Use of a biomimetic strategy to engineer bone. Journal of biomedical materials research. Part A. 2003/06/15, 65, 447-453. DOI: 10.1002/jbm.a.10453

[114] ITÄLÄ, A.; YLÄNEN, H.; EKHOLM, C.; et al.: Pore diameter of more than 100 μm is not requisite for bone ingrowth in rabbits. Journal of biomedical materials research. 2001/02/01, 58, 679-683. DOI: 10.1002/jbm.1069

[115] CIZEK, J.; KHOR, K.: Role of In-Flight Temperature and Velocity of Powder Particles on Plasma Sprayed Hydroxyapatite Coating Characteristics. Surface and Coatings Technology. 2012/01/15, 206, 2181-2191. DOI: 10.1016/j.surfcoat.2011.09.058

[116] VU, T. A.; HEIMANN, R. B.: Improvement of the Adhesion Strength of Plasma-Sprayed Bioceramic Coatings, DVS Berichte, 1996, 175, 178-181

[117] GROSS, K.; SABER-SAMANDARI, S.: Revealing Mechanical Properties of a Suspension Plasma Sprayed Coating with Nanoindentation. Surface and Coatings Technology. 2009/07/01, 203, 2995-2999. DOI: 10.1016/j.surfcoat.2009.03.007

[118] YI, J.; SONG, L.; LIU, X.; et al.: Hydroxyapatite Coatings Deposited by Liquid Precursor Plasma Spraying: Controlled Dense and Porous Microstructures and Osteoblastic Cell Responses. Biofabrication. 2010/11/01, 2, 045003. DOI: 10.1088/1758-5082/2/4/045003

[119] BORISOV, Y.; Borisova, A. L.; Tuniket, A. Y.; et al.: Effect of microplasma spray conditions on structure, phase composition and texture of hydroxyapatite coatings. Thermal Spray 2006: Building on 100 Years of Success, 2006, 29-34.

[120] DEMNATI, I.; PARCO, M.; GROSSIN, D.; et al.: Hydroxyapatite coating on titanium by a low energy plasma spraying mini-gun. Surface and Coatings Technology. 2012/01/15, 206, 2346-2353. DOI: 10.1016/j.surfcoat.2011.10.025

[121] LIU, X.-M.; HE, D.; ZHOU, Z.; et al.: Atmospheric Plasma-Sprayed Hydroxyapatite Coatings with (002) Texture. Journal of Thermal Spray Technology. 2018/10/12, 27. DOI: 10.1007/s11666-018-0768-1

[122] CIZEK, J.; BROZEK, V.; CHRASKA, T.; et al.: Silver-Doped Hydroxyapatite Coatings Deposited by Suspension Plasma Spraying. Journal of Thermal Spray Technology. 2018/10/12, 27. DOI: 10.1007/s11666-018-0767-2

7 List of symbols and abbreviations

Symbols

α [1/K]	Thermal expansion
λ [W/m.K]	Thermal conductivity
ρ $[g/cm^3]$	Density
E [GPa]	Young's modulus
HRC	Hardness Rockwell C
R_a $[\mu m]$	Arithmetical mean roughness
R_e [MPa]	Yield strength
R_m [MPa]	Ultimate tensile strength
R_z $[\mu m]$	Mean roughness depth
T_m [°C]	Melting temperature

Abbreviations

APS	Atmospheric plasma spray
ACP	Amorphous calcium phosphate
BCC	Body centered-cubic
CAPS	Controlled atmosphere plasma spray
CCP	Capacitively-coupled plasma
CVD	Chemical vapor deposition
DC	Direct current
D-Gun	Detonation gun
FDA	Food and Drug Administration
HA	Hydroxylapatite
HCP	Hexagonal close-packed
HVAF	High-velocity air fuel
HVOF	High-velocity oxygen fuel
ICP-AES	Inductively-coupled plasma - atomic emission spectrometry

ICP-MS	Inductively-coupled plasma - mass spectrometry
ICP-OES	Inductively-coupled plasma - optical emission spectrometry
ICP-RIE	Inductively-coupled plasma - reactive-ion etching
IPP	Institute of Plasma Physics
IPS	Inert plasma spray
ISM	Industrial, scientific and medical
LEPS	Low-energy plasma spray
LPPS	Low pressure plasma spray
MAPP	Methylacetylene-propadiene propane
MIPS	Microplasma spray
OA	Oxyapatite
OHA	Oxyhydroxylapatite
PEG	Polyethylene glycol
PLGA	Polylactic-co-glycolic acid
PMMA	Polymethyl methacrylate
PVA	Polyvinyl alcohol
PVD	Physical vapor deposition
RF-ICP	Radio frequency inductively-coupled plasma
SEM	Scanning electron microscope
SPPS	Solution precursor plasma spray
SPS	Suspension plasma spray
TCP	Tricalcium phosphate
TTCP	Tetracalcium phosphate
VPS	Vacuum plasma spray
WSP-H	Hybrid water/gas stabilized plasma
XRD	X-ray diffraction